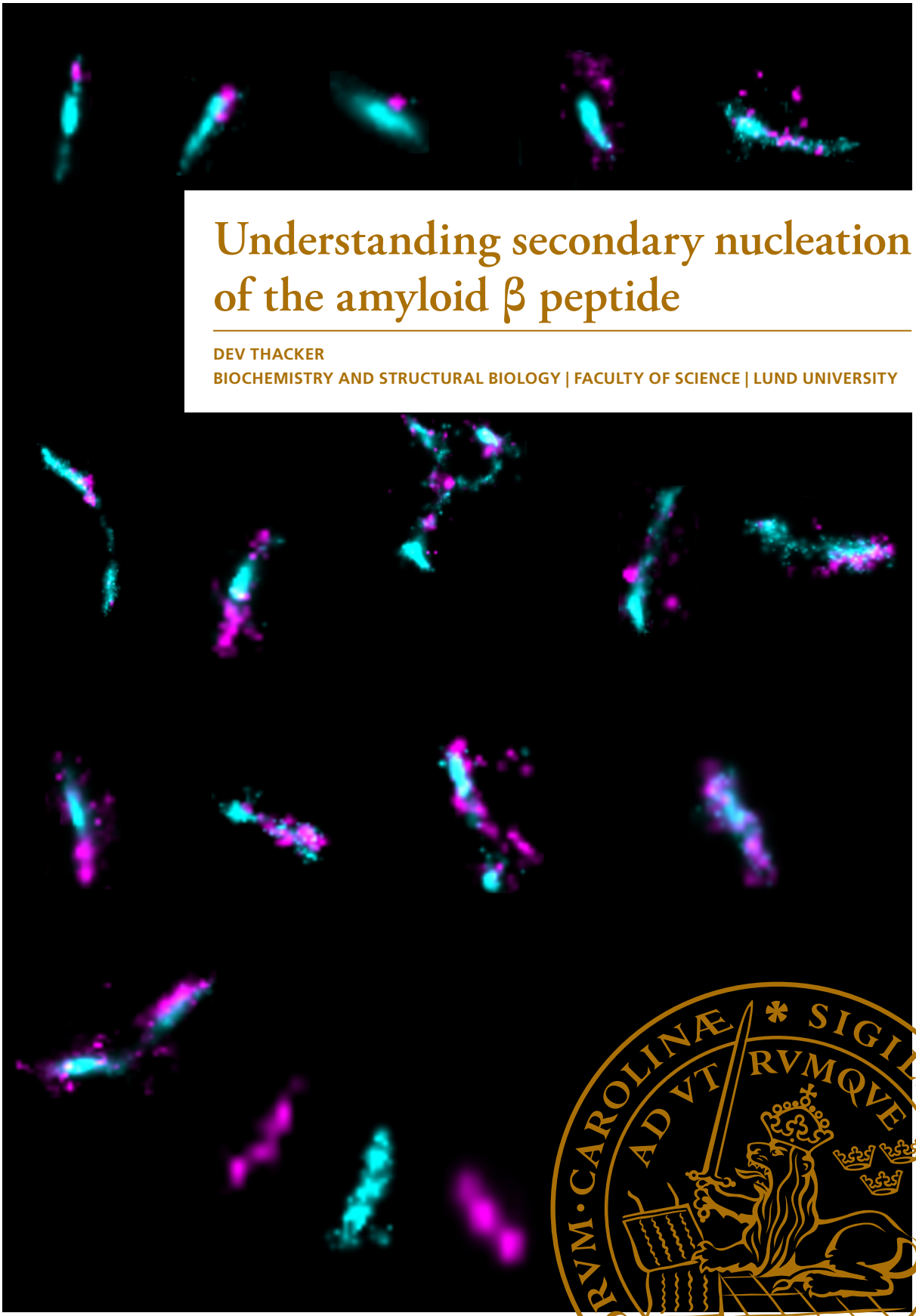

Understanding secondary nucleation of the amyloid β peptide

DEV THACKER
BIOCHEMISTRY AND STRUCTURAL BIOLOGY | FACULTY OF SCIENCE | LUND UNIVERSITY

Keep Ithaka always in your mind.
Arriving there is what you're destined for.
But don't hurry the journey at all.
Better if it lasts for years,
so you're old by the time you reach the island,
wealthy with all you've gained on the way,
not expecting Ithaka to make you rich.

Ithaka gave you the marvelous journey.
Without her you wouldn't have set out.
She has nothing left to give you now.

And if you find her poor, Ithaka won't have fooled you.
Wise as you will have become, so full of experience,
you'll have understood by then what these Ithakas mean.

- *Ithaka,* C. P. Cavafy.

Printed by Media-Tryck, Lund 2022 NORDIC SWAN ECOLABEL 3041 0903

LUND UNIVERSITY

Biochemistry and Structural Biology
Faculty of Science
Lund University

ISBN 978-91-7422-860-1

Understanding secondary nucleation of the amyloid β peptide

Understanding secondary nucleation of the amyloid β peptide

by Dev Thacker

LUND
UNIVERSITY

Thesis for the degree of Doctor of Philosophy
Thesis advisors: Prof. Sara Linse, Assoc. Prof. Peter Jönsson, Martin Lundqvist
Faculty opponent: Prof. Louise Serpell

To be presented, with the permission of the Faculty of Science of Lund University, for public criticism in lecture hall A at the Center for Chemistry and Chemical Engineering on Wednesday, the 9th of March 2022 at 09:15.

Organization
LUND UNIVERSITY
Biochemistry and Structural Biology
Box 124
SE–221 00 LUND
Sweden

Document name
DOCTORAL DISSERTATION

Date of disputation
2022-03-09

Sponsoring organization

Author(s)
Dev Thacker

Title and subtitle
Understanding secondary nucleation of the amyloid β peptide:

Abstract
Alzheimer's Disease (AD) is a devastating neurodegenerative disease associated with massive neuronal cell death during its pathology. The involvement of the amyloid β 42 (Aβ42) peptide and its role in neurotoxicity is now well established. It is known that the production of oligomers during the aggregation of Aβ42 into highly ordered fibrils is responsible for neuronal cell death. However, the efforts in finding a cure have been greatly hindered because of the lack of understanding of the molecular mechanisms of Aβ42 aggregation. This thesis focuses on understanding the molecular mechanism of secondary nucleation, the process which is most prolific in the production of oligomers. In particular, the work focuses on intrinsic factors affecting secondary nucleation such as hydrophobic residues and surfaces on the fibrils, which catalyze the aggregation of monomers during secondary nucleation. We also show the possibility of molecular specificity being involved in secondary nucleation, and open avenues of further studies that will help understand the molecular mechanism of this phenomenon.

Key words
Alzheimer's disease, Amyloid aggregation, Aβ42, Secondary nucleation.

Classification system and/or index terms (if any)

Supplementary bibliographical information

Language
English

ISSN and key title

ISBN
978-91-7422-860-1 (print)
978-91-7422-861-8 (pdf)

Recipient's notes

Number of pages
194

Price

Security classification

Understanding secondary nucleation of the amyloid β peptide

by Dev Thacker

LUND
UNIVERSITY

Author photo.

Cover illustration front: Picture by the author. Nucleation and growth events in Aβ42 aggregation as observed by dSTORM.

Cover illustration back: Picture by the author. Poem: Ithaka, by C. P. Cavafy.

Faculty of Science, Biochemistry and Structural Biology

ISBN: 978-91-7422-860-1 (print)
ISBN: 978-91-7422-861-8 (pdf)

Printed in Sweden by Media-Tryck, Lund University, Lund 2022

NORDIC SWAN ECOLABEL
Printed matter
3041 0903

Media-Tryck is an environmentally certified and ISO 14001:2015 certified provider of printed material. Read more about our environmental work at www.mediatryck.lu.se

MADE IN SWEDEN

Dedicated to my mother

Contents

List of publications

This thesis is based on the following publications, referred to by their Roman numerals:

I **The role of fibril structure and surface hydrophobicity in secondary nucleation of amyloid fibrils**
D. Thacker, K. Sanagavarapu, B. Frohm, G. Meisl, T. P. J. Knowles, S. Linse
PNAS, volume 117, article 41 (2020).

II **Role of hydrophobicity at the N-terminal region of Aβ42 in secondary nucleation**
D. Thacker, A. Willas, A. J. Dear, S. Linse
Manuscript

III **A palette of fluorescent Aβ42 peptides labelled at a range of surface-exposed sites**
D. Thacker* and M. Bless*, M. Barghouth, E. Zhang, S. Linse
Accepted in Int. J. Mol. Sci

IV **Direct observation of secondary nucleation along fibril surfaces of Aβ42 from direct stochastic optical reconstruction microscopy (dSTORM)**
D. Thacker, M. Barghouth, M. Bless, E. Zhang, S. Linse
Manuscript

*These authors contributed equally to the article.

List of publications not included in thesis

I **The catalytic nature of Aβ oligomer formation and dissociation**
A. Dear, **D. Thacker**, S. Linse, T. P. J. Knowles
Manuscript

II **The effect of DNAJB6 on α-synuclein aggregation in vitro**
T. Pâlmadóttir, **D. Thacker**, M. Oosterhuis, C. Emanuelsson, S. Linse
Manuscript

III **Effects on aggregation kinetics and interactions with Aβ42 of the functionally important C-terminal region of the anti-amyloid chaperone DNAJB6**
N. Österlund, R. Frankel, A. Carlsson, **D. Thacker**, M. Karlsson, V. Matus, C. Emanuelsson, S. Linse
Manuscript

My contribution to the papers

Paper I: The role of fibril structure and surface hydrophobicity in secondary nucleation of amyloid fibrils

I took part in purification of the proteins. I performed the aggregation kinetics experiments. I performed the ANS fluorescence experiments. I prepared samples for cryoTEM. I took part in the data analysis. I wrote the first draft of the manuscript.

Paper II: Role of hydrophobicity at the N-terminal region of Aβ42 in secondary nucleation

I took part in the design of the study. I took part in purification of the proteins. I took part in the aggregation kinetics experiments. I prepared samples for, and performed the cryoTEM imaging. I took part in the data analysis. I wrote the first draft of the manuscript.

Paper III: A palette of fluorescent Aβ42 peptides labelled at a range of surface-exposed sites

I took part in the design of the study. I took part in purification of the proteins. I took part in the aggregation kinetics experiments. I took part in preparation of samples, and performed cryoTEM imaging. I took part in data analysis. I wrote the first draft of the manuscript.

Paper IV: Direct observation of secondary nucleation along fibril surfaces of Aβ42 from direct stochastic optical reconstruction microscopy (dSTORM)

I took part in the design of the study. I took part in the purification of the proteins. I took part in the preparation of samples for dSTORM. I took part in the dSTORM imaging. I took part in data analysis. I wrote the first draft of the manuscript.

Acknowledgements

I am filled with immense gratitude as I even begin to write this. It has been the most wonderful journey and I am so happy to have shared it with some amazing people.

First and foremost I would like to thank my supervisor. **Sara**, five years back I wrote to you that I want just want to do the work that I love in peace. Thank you for giving me the chance to do that in your group. It has been an inspiration seeing you in the lab everyday excited about experiments, and enjoying the science. The way you treat everyone around you with kindness and patience is exemplary. Thank you for being supportive throughout these years and always encouraging me to learn new things. I could not have enjoyed my time as a PhD student more!

Martin, thank you for helping me get settled to life at KC, and for always being there whenever I needed help, and also for sharing my sorrows over our football team.

Thanks to all the members - past and present- of my family away from home - SSLRGLU. My office mates - **Egle**, thank you for being a great office mate (reminding me of the salary increments) and friend, and for sharing my troubles over teaching; **Rebecca**, for patiently guiding me through the thesis writing process, for being a great office mate and friend, and for our awesome gingerbread house; **Tinna** for being a great friend and a warm presence in the lab, and for always making our conference trips so much fun. **Mattias**, for your delightful sense of humor and for providing a much needed laugh while dealing with this darn peptide of ours, **Marija**, for sharing this journey with me right from the beginning, for our amazing trip to Kiruna, and for all the coffees in the sun, **Caroline**, for always reminding me to take a break, and for exploring all the restaurants in Malmö with me. **Kalyani** thank you for helping me get settled in the lab and for all the great advice over the years, and for the project we shared together, **Xiaoting**, for being so warm and friendly when I was a nervous newbie in the lab, **Tanja**, for all the nice chats, and all the WT Aβ, **Veronica**, for all your energy and happy smiles in the lab, **Lei**, for our efforts to make PICUP work for Aβ and for all the discussions about football, **Diana** for bringing such positive energy every time you visit, and for giving me a great burrito recipe, **Thom** and **Birgitta**, for always keeping things running smoothly in the lab and allowing us to thrive, **Katja**, for all your positive energy and smiles, **Ricardo**, it was really great having you around in the lab and listening

to your stories about your experience in football, **Karin Åkerfeldt**, it is always so great to have you around every time you visit, you always manage to lift our spirits and spread joy, **Eimantas**, for being a great office-mate and for always patiently helping me with everything, **Kasia**, for all the engaging scientific discussions and conversations, **Christin**, for all the fun conversations during cryoEM sessions, **Emil, Max, Jing,** and **Andreas**, thank you for bringing new energy to the group and opening up new topics of discussions! My students **Amanda** and **Mara**, I enjoyed sharing some fun and fruitful research projects with you, you helped me become a better researcher.

A big thanks to all the members of CMPS for creating a lovely workplace. **Tommy** and **Susanna**, for the new leadership at CMPS, **Magnus**, for putting up with us and for everything you do in keeping the department running smoothly, **Maryam**, for organizing fikas and get-togethers that spread so much joy, **Urban** and **Cecilia**, for all the support during teaching over the years, **CJ** and **Camille**, for being great teaching-buddies and making the experience more fun. Special mentions to **Johan, Sven, Olof, Filip, Zhiwei, Santosh, Ashhar, Bhakat, Signe, Mads, Kristine, Tamim, Helin, Jennifer, Veronika, Simon, Mathias, Samuel, Rohit, Ipsita, Isabella, Shanti**, for creating such a great environment at the department, for all the lovely discussions about science, and life in general, for all the laughs, the Christmas parties, barbecues, and beer clubs. **Abhishek**, for bringing me food when I broke my hand, I couldn't have survived without you, but more importantly for sharing my sorrows over our football team. **Mandar** and **Ramya**, thank you for being my family here, for all the PlayStation battles, for looking after me when I broke my hand, and for our trip to Rugen, I hope we are in the same corner of the world again soon.

My cryoEM mentors, **Anna** and **Crispin**, thank you for helping me learn this fascinating technique. Thanks as well to **Markel** and **Emil**, for guiding me as I take steps into single particle analysis.

All my collaborators - **Georg** and **Alex**, the data analysis wizards, **Mohammad** and **Enming** for all your help with dSTORM, **Stefan**, for being so patient during our FCS experiments and some really enjoyable conversations.

To my doctor **Anna-Kajsa**, my physiotherapist **Benjamin**, and my occupational therapist **Ronja**, a big thank you for everything you did to help me with my broken arm. You literally have a hand in all the work I've done

since then.

Mom, there is no way I could have done it without you. All the sacrifices you made, all your unwavering support in helping me achieve my dreams and being there for me in the darkest times, this is yours as much as it is mine. I love you. **Bhupen masa**, thank you for all the support, advice, and guidance, I really appreciate it. **Dhaara**, thank you for being patient with me while I wrote this book. Congratulations on your new job, I'm really excited about the future. **Grandma**, and **grandpa**, I wish you were here to see me finish my thesis, thank you for always believing in me, even during the times when I did not.

Popular Science Summary

Imagine you are going out on a Friday night for dinner. But you are new in town and don't know any of the good places. You see a restaurant which is completely empty with no customers inside eating food. If this place was good, wouldn't there be some people in there? You hesitate to go in. You walk a little bit further and see a restaurant which is full of people! Well, this one must be good, so many people are eating there! You have no hesitation in going and standing in the queue. This behaviour is not just seen in humans but in all aspects of nature. Crystals and nanoparticles have been known to grow on already existing aggregates more easily than forming a completely new one on their own. Even particles of pollution in the atmosphere tend to join a larger cluster of particles rather than float around on their own. Inside our own body, biomolecules called proteins show this behavior as well. Some proteins tend to aggregate, together creating larger assemblies. However, for proteins, it is easier to join an already existing assembly as compared to starting their own assembly.

Let's talk about proteins a little bit more. These are very important molecules in our body that are essential in performing crucial functions. Indeed, our body could not survive without them. Some proteins are messengers between cells, some fight infections in our body and keep us healthy, and so on. However, during some diseases, certain proteins can actually be harmful to the body. One such disease is Alzheimer's disease. This disease is normally associated with age, but in some cases, it has an early onset at a younger age as well. It is a neurodegenerative disease, which means that along with its progression, degeneration of the brain and its functioning occurs. The cognitive senses of the patient decline, it becomes difficult for the patient to take care of themselves and perform basic daily tasks such as maintaining hygiene, they experience memory loss, there is massive neuronal cell death, and the volume of their brain shrinks. A large reason behind all these symptoms is a small protein called amyloid β peptide, or Aβ. Aβ exists as variants of different lengths. One such variant is Aβ42, which is 42 amino acids long. During the pathology of Alzheimer's, Aβ42 becomes neurotoxic. Turns out, Aβ42 also likes to aggregate to larger assemblies, like the other particles in nature. These larger aggregates have been found in the brains of Alzheimer's patients. It is somewhere during this process of aggregation that Aβ42 adopts a highly neurotoxic structure.

Let's go back to the original analogy again of forming a queue outside the restaurant. You are walking in the town looking for a restaurant to eat at.

Outside one restaurant you see a group of your friends waiting in the queue, and outside another restaurant you see a bunch of strangers. You go and join your friends for dinner of course! Do proteins show this behavior when joining a larger assembly as well? Do they go to an assembly where they see familiar features that they can recognize and prefer it over assemblies that have no such features? Let's really stretch this analogy, because why not. You are standing in the queue outside the restaurant with your friends. Now you are a big group and there might not be space for you inside. At some point you all decide to leave the queue and go get food somewhere else. Do proteins growing on assemblies do this as well? At what point does a cluster of protein molecules separate from a larger aggregate and go form their own aggregate? Knowing the answers to these questions will help us understand protein behavior better, and so these are some of the questions we try to answer in this thesis. If we understand this protein aggregation behavior better, we can design a better approach to cure diseases.

We hope that one day we know enough about these proteins that we can find a cure for Alzheimer's, such that there is no protein aggregation in the brain, just like there were no queues outside restaurants during the COVID19 pandemic.

1

Alzheimer's Disease

"The woods are lovely, dark and deep, but I have promises to keep.
And miles to go before I sleep, and miles to go before I sleep..."

- *Stopping by the woods on a snowy evening*, Robert Frost

1.1 Background

In 1907 Alois Alzheimer wrote an article reporting a peculiar case. The director of the insane asylum of Frankfurt am Main gave him a specimen of a patient's central nervous system for clinical analysis. The case could not be classified as any recognized illness, as the clinical analysis showed anatomical characteristics that set it apart from other cases [1]. The patient was Auguste Deter, a 55-year-old woman who had died from a progressive behavioral and cognitive disorder. Alzheimer was convinced that the case of Auguste Deter represented an unusual cause of dementia. Since then, Alzheimer's Disease (AD), which this illness later came to be known as, has been recognized as the leading contributor of dementia, accounting for up to 75% of the cases [2]. It is estimated that approximately 47 million people over the world are currently living with dementia, and this number is projected to be 90 million by 2030 [3]. According to the WHO data published in 2018, Alzheimer's caused deaths in Sweden accounted for 12.55% of total deaths.

AD is a progressive neurodegenerative disease and affects the cerebral cortex and hippocampus [4]. The most common early symptom is difficulty remembering recent events (short-term memory loss). As the disease advances, symptoms can include problems with language, disorientation (including easily getting lost), mood swings, loss of motivation, not managing self-care, and behavioural issues. A hallmark of AD pathology is the deposition of amyloid proteins in the form of neurofibrillary tangles and senile plaques in patient brains.

While age is the factor most closely related to AD, several other factors have been known to increase the risk of developing Alzheimer's. These include cerebrovascular disease [5–7], hypertension [8, 9], diabetes [10, 11], obesity [12], smoking [13], and traumatic brain injury [14]. Recently there has also been growing evidence that sleep disturbance is strongly linked with AD [15]. Approximately 25–66% of AD patients exhibit sleep disturbances [16, 17]. On top of these, the involvement of various genetic factors is also known to cause an early onset and rapid progression of the disease. However, there are also some factors that seem to have a protective effect against AD. For example, lower cases of AD in people with higher education has been reported [18–21]. Community activities, social engagements, and leisure activities that count as intellectual exercises have also been reported as protective against AD [22–24]. Apart from these, a healthy diet and physical activity are also shown to have a protective role against AD [25,

26].

While the very first drug to treat AD has recently received Food and Drug Administration (FDA) approval, there is a large room for improvement. Understanding the molecular mechanism of the disease will only help in designing a more efficient cure.

1.2 Amyloid Cascade Hypothesis

In 1907, Alois Alzheimer reported the presence of a "peculiar substance" in the central nervous system sample of Auguste Deter, but it was only in 1984 that this was identified as the amyloid β (Aβ) peptide [27]. In 1992, the amyloid cascade hypothesis was proposed by JA Hardy and GA Higgins [28]. The amyloid cascade hypothesis states that the deposition of amyloid β peptide is the causative event of Alzheimer's disease and that neurofibrillary tangles, cell loss, vascular damage, and dementia follow as a direct result of this deposition. Aβ was identified as the main component of senile plaques [4, 27]. Aβ is derived from the cleavage of a transmembrane protein, *amyloid precursor protein* (APP) [29]. The main component of the neurofibrillary tangles was identified to be the protein tau [30], a key component for microtubule assembly in axons [31].

Both Aβ and tau are amyloid proteins and form highly ordered fibrillar aggregates. While these fibrillar aggregates were initially considered to be the neurotoxic species in AD, this opinion has changed over the years. It has since then been established that the fibrils of these amyloid proteins are relatively inert, while it is the intermediate aggregate species that are neurotoxic [32].

While the amyloid cascade hypothesis has been recently challenged [33, 34], a major form of support comes from the discovery that individuals with Down's syndrome, who have a duplication of chromosome 21 and thus over-express the gene for APP, have significantly higher chances of getting Alzheimer's disease [35]. More support has come from studies showing that APP transgenic mouse models exhibit some of the main pathological signs of AD, such as the formation of Aβ plaques, synaptic loss, synaptic plasticity alterations, and memory impairment [36].

2

The Amyloid β Peptide

"..If you can meet with Triumph and Disaster

And treat those two impostors just the same..."

- *If*, Rudyard Kipling

The Aβ peptide exists as variants of different lengths, based on the total number of amino acids in its sequence. Out of these variants, Aβ40 (40 amino acids) is present at higher concentrations in the brain, but Aβ42 (42 amino acids) is more aggregation-prone and thus linked more closely to the disease [37]. As mentioned in Chapter 1, Aβ42 is generated by the cleavage of a larger transmembrane protein, APP. APP is cleaved by β-secretase before Asp1 residue of the Aβ-domain [7]. Subsequent proteolysis by γ-secretase gives rise to a variation of length variants at the C-terminus [38–40]. This thesis focuses on Aβ42. In its native form, Aβ42 is monomeric and unstructured. During the pathology of Alzheimer's disease, Aβ42 undergoes an aggregation process and forms highly ordered amyloid aggregates through a series of microscopic steps. The nature of this self-assembly process can be described as auto-catalytic. It is during this self-assembly process that the intermediate neurotoxic species appear, and hence it is important to study the mechanism of aggregation.

2.1 Mechanism of Aβ42 aggregation

Over the last few years, significant progress has been made in understanding the aggregation mechanism of Aβ42. This has been made possible thanks to improved techniques to gain reproducible data on aggregation kinetics of Aβ42 [41], as well as the development of mathematical kinetic models [42, 43]. The most common method to study the aggregation of amyloid proteins such as Aβ42 is to follow the fluorescence of a dye called Thioflavin T (ThT), which binds specifically to amyloid structures (see Chapter 3 for more details). It is now established that the self-assembly process involves a series of microscopic steps, namely primary nucleation, elongation, and secondary nucleation. Primary nucleation involves monomers only, while secondary nucleation and elongation involve fibrils and monomers both.

2.1.1 Primary Nucleation and Elongation

A typical ThT fluorescence assay for following the aggregation of Aβ42 consists of an initial lag phase, followed by an exponential phase, and a final plateau. This reflects the formation of ThT-positive amyloid structures from the starting monomer solution. Primary nucleation dominates the early lag phase of this ThT curve (figure 2.2) [44]. This is a slow process. Close to the very beginning of the aggregation reaction, just after t=0, when

there are no species of aggregates present, primary nucleation is the only active molecular event, while fibril dependent processes like elongation and secondary nucleation are completely suppressed [44]. Monomers in bulk solution form primary nuclei. Once a nucleus is formed, it can continue growing through elongation (figure 2.1). In elongation, monomers are added to fibril ends and take up the structure of the parent fibril. The energy barrier for elongation is lower than for primary nucleation, and it is a faster process. Soon, secondary nucleation can start occurring.

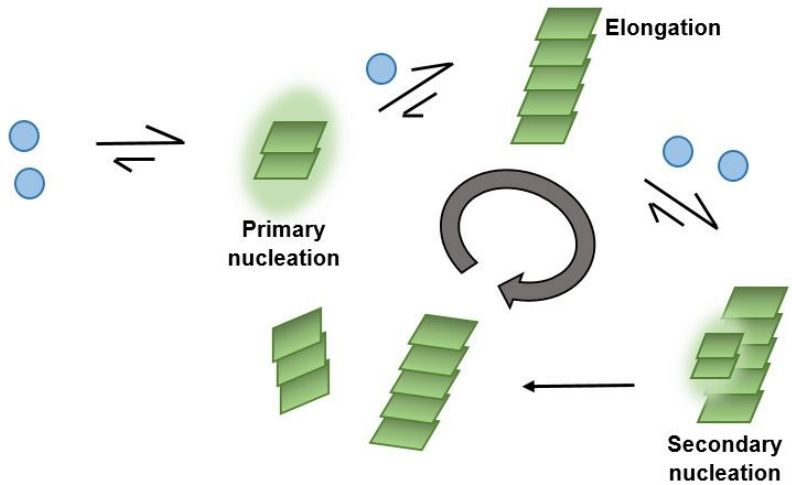

Figure 2.1: Microscopic steps involved in autocatalytic proliferation of Aβ42. Blue circles represent monomers, and green squares represent nuclei and growing aggregates.

2.1.2 Secondary Nucleation

Remarkably, nucleated growth processes are everywhere around us in nature. Crystals [45], nanoparticles [46], and even particulate matter in air pollution [47] have been shown to grow by nucleation processes. This is such a common phenomenon because the energy barrier for growing on a pre-existing aggregate is lower than that for starting a new aggregate.

In the amyloid aggregation process, once primary nuclei are formed, they can grow through elongation, but they can also provide a surface to catalyze the growth of more monomers and the formation of new nuclei on their surface. These nuclei can then detach from the fibril surfaces, grow through elongation, and further provide a surface for the formation of more nuclei

(figure 2.1). This process is thus autocatalytic in nature and is responsible for the exponential growth phase in the ThT fluorescence curve (figure 2.2) [42]. Given this exponential growth phase, secondary nucleation produces substantially more oligomeric aggregates compared to the other growth processes. It has been established now that these oligomers are the neurotoxic species in Alzheimer's disease [48–50].

The rate of secondary nucleation is dependent on both monomers and fibrils. In some cases, it has been observed that secondary nucleation is saturated [51, 52]. In this situation, all available fibril surfaces are completely covered by monomers, leaving no more space for the attachment of more monomers and the formation of new nuclei until the nucleated species on the fibril surfaces are detached.

Another process worth mentioning is fragmentation, which involves breaking off of fibrils and thus the creation of more fibrillar ends for the growth of monomers through elongation. This creates a sharp increase in the growth rate. Fragmentation can be influenced by extrinsic factors such as agitation.

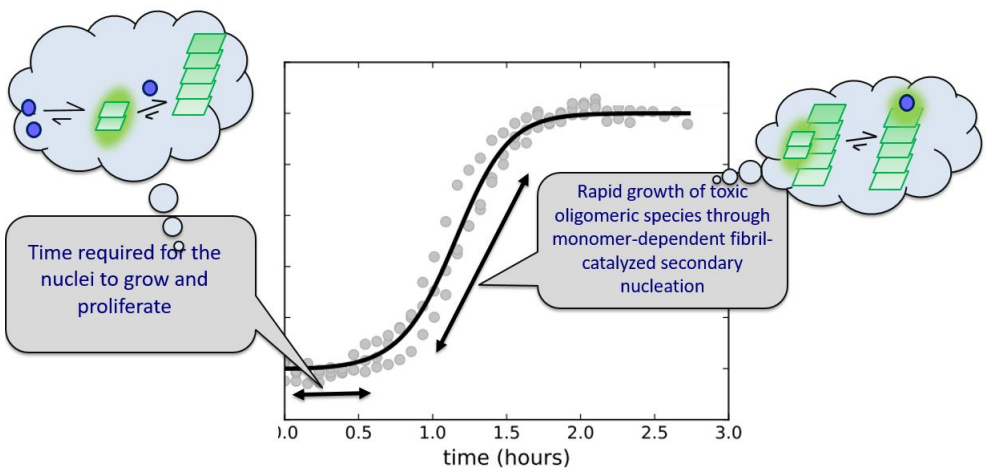

Figure 2.2: A typical ThT assay curve for Aβ42 and the dominant processes in it. All the microscopic steps involved in the self-assembly of Aβ42 are ongoing simultaneously in all phases of the sigmoidal curve, but certain processes are the driving forces during certain phases.

After the early primary nuclei are formed, all microscopic processes - primary nucleation, elongation, and secondary nucleation - occur simultaneously during all phases of the growth curve until the free monomers in the solution are depleted.

This mechanism of secondary nucleation dominated proliferation is also observed for Aβ40 [51], and other amyloid proteins involved with disorders such as α-synculein in Parkinson's Disease [53], and IAPP in type II diabetes [54].

2.1.3 Oligomers

As mentioned earlier, it has now been established that oligomers are the neurotoxic species during Alzheimer's disease, while fibrils are relatively inert. While there is no doubt that oligomers are also generated during primary nucleation, the generation of oligomers is much more prolific during secondary nucleation due to the catalytic surfaces provided by fibrils. As a result, we see a similarly sharp increase in oligomer formation as we do with fibril formation followed by ThT fluorescence (figure 2.3). Indeed, targeting secondary nucleation of Aβ42 has been shown to reduce the toxicity of the peptide *in vivo* by lowering oligomer formation [55]. However, oligomers are transient species, and their concentration decreases over time [56].

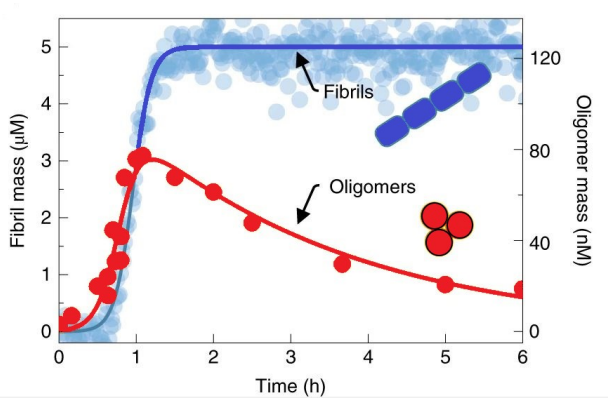

Figure 2.3: Evolution of oligomer concentration over the aggregation time-scale as followed by liquid scintillation counting. Figure adapted from ref. [56].

Notably, the decrease in oligomer concentration is much slower compared to the sharp increase in oligomer formation at the beginning of the aggregation reaction. This decrease of oligomer concentration can in part be attributed to their conversion into fibrils, but a large number of oligomers also dissociate back to monomers without being converted into fibrils [56].

The transient nature of oligomers has made detailed studies challenging and structural information about oligomers is limited. Structures of oligomers

that have been stabilized by sodium dodecyl sulfate (SDS), or by other detergent micelles are available [57–59]. The limited structural information about oligomers makes it even more important to understand the molecular mechanism of secondary nucleation and oligomer formation in order to develop a targeted approach for curing Alzheimer's disease.

2.1.4 Rate Constants

Mathematical terms can be assigned to these microscopic steps involved in the aggregation process. Doing this can help us understand how the system can evolve over time.

Before we begin with the mathematical equations for the nucleation processes, let's define some variables to understand them. During the aggregation process, at a given time, the system will contain:

m(t) - the concentration of free monomers,

M(t) - the mass concentration of fibrils,

P(t) - the number concentration of fibrils.

As discussed earlier, at the beginning of the reaction process, closer to t=0, fibril dependent processes like elongation and secondary nucleation will be inactive because M(t) and P(t) will be zero. The value of m(t) at t=0 will be whatever initial monomer concentration that we start the experiment with (m(0)). At this time, primary nucleation will be the first active process, generating new fibrils at a rate described as:

$$\frac{\delta P}{\delta t} = k_{\mathrm{n}} m(t)^{n_c},$$

where, k_n is the primary nucleation rate constant, and n_c is the primary nucleation order.
The process consumes monomers and adds to the fibril mass, but this contribution is small enough to be neglected. Instead, the process which is the main contributor to fibril mass by monomer addition is elongation, which can be described as:

$$\frac{\delta M}{\delta t} = k_{+} m(t) P(t)$$
$$\frac{\delta m}{\delta t} = -k_{+} m(t) P(t),$$

where k_+ is the elongation rate constant.

The nuclei that have grown through elongation act as catalytic surfaces during secondary nucleation for the growth of more monomers and the production of new fibrils, which can be described as:

$$\left(\frac{\delta P}{\delta t}\right)_{\text{sec}} = k_2 m(t)^{n_2} M(t),$$

where k_2 is the secondary nucleation rate constant, and n_2 is the secondary nucleation reaction order.

The processes described by these equations all contribute to the production of new fibrils over time. In order to determine the contribution of each process to the production of new fibril mass over time, and to determine the individual rate constants, rate equations have been solved to create a master equation describing time evolution of fibril mass [60]:

$$\frac{M(t)}{M_\infty} = 1 - \left(\frac{B_- + C_+ e^{\kappa t}}{B_+ + C_+ e^{\kappa t}} \cdot \frac{B_+ + C_+}{B_- + C_+}\right)^{\frac{\alpha^2}{\kappa\beta}} \cdot e^{-\alpha t},$$

where the definitions of the parameters are

$$\lambda = \sqrt{2k_+ k_{\text{n}} m(0)^{n_{\text{c}}}}$$

$$\kappa = \sqrt{2k_+ k_2 m(0)^{n_2+1}}$$

$$B_\pm = \frac{\alpha \pm \beta}{2\kappa}$$

$$C_\pm = \pm\frac{\lambda^2}{2\kappa^2}$$

$$\alpha = \sqrt{\frac{2\kappa^2}{[n_2(n_2+1)] + \frac{2\lambda^2}{n_{\text{c}}}}}$$

$$\beta = \sqrt{\alpha^2 - 4C_+ C_- \kappa^2}$$

where P_∞ and M_∞ are the aggregate number and mass concentration at the end of the aggregation reaction.

This equation and expansions of it have helped us extract individual rate constants and the effects of various conditions on them, and thus understand the aggregation mechanism. The online platform Amylofit [43] was developed to facilitate this, where we can upload experimental data and analyze by global fitting of various models.

Saturated secondary nucleation:

As explained earlier, secondary nucleation can sometimes be saturated, for example, at high peptide concentrations. Saturation of nucleation processes can be explained in a similar manner to Michaelis Menten kinetics. The rate of formation of new fibrils with saturated secondary nucleation can be described as:

$$\frac{\delta P}{\delta t} = k_2 M(t) \cdot \frac{m(t)^{n_2}}{1 + \frac{m(t)^{n_2}}{K_\mathrm{M}}}$$

Where K_M is the saturation constant for secondary nucleation.

The master equation is then adapted to [60]:

$$\frac{M(t)}{M_\infty} = 1 - \left(1 - \frac{M(0)}{M_\infty}\right) e^{-\alpha t} \cdot \left(\frac{B_- + C_+ e^{\kappa t}}{B_+ + C_+ e^{\kappa t}} \cdot \frac{B_+ + C_+}{B_- + C_+}\right)^{\frac{\alpha^2}{\kappa\beta}},$$

where the definitions of the parameters are

$$\lambda = \sqrt{2 k_+ k_\mathrm{n} m(0)^{n_\mathrm{c}}}$$

$$\kappa = \sqrt{2 m(0) k_+ \cdot \frac{m(0)^{n_2} k_2}{1 + m(0)^{n_2}/K_\mathrm{M}}}$$

$$B_\pm = \frac{\alpha \pm \beta}{2\kappa}$$

$$C_{\pm} = \frac{k_+ P(0)}{\kappa} \pm \frac{k_+ M(0)}{2m(0)k_+} \pm \frac{\lambda^2}{2\kappa^2}$$

$$\alpha = 2k_+ P_\infty$$

$$\beta = \sqrt{\alpha^2 - 4C_+ C_- \kappa^2}$$

This mathematical model of saturating secondary nucleation is used to fit experimental data for some of the peptides studied in this thesis, and the kinetic analyses of experiments are performed with the help of our collaborators *G. Meisl, A. Dear*, and *T. P. J. Knowles*.

2.2 Fibril Structure

Understanding the structure of Aβ42 fibrils is key in deciphering the molecular mechanism of secondary nucleation. Several high resolution structures of the Aβ42 fibril core have been solved [61–63]. One of these [62] is shown in figure 2.4. Each fibril consists of two filaments, which in turn are built by a large number of monomer planes stacked on top of each other, perpendicular to the fibril axis. Each plane in a filament consists of two monomer units. The first 14 amino acid residues of Aβ42 constitute the N-terminal region, which remains relatively flexible in the end-stage fibrils. The residues 15-42 form the fibril core. Contrasting structures of Aβ42 fibrils have also been reported, hinting that the fibril structure is strongly influenced by sample conditions [64–67].

In typical Aβ42 aggregates, individual filaments can be observed, and two filaments are twisted around each other along a common axis, seen as "nodes" that appear along the fibril at regular intervals. This can be observed in the fibril morphology from cryoTEM images (figure 2.4 (A)). The distances between these periodical nodes can be calculated from cryoTEM images. These node-to-node distances have been used to characterize different morphologies for fibrils formed by various Aβ42 mutants studied in this thesis.

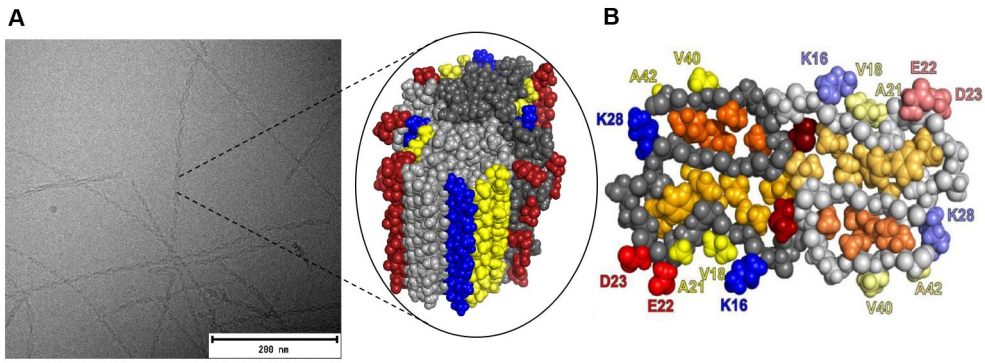

Figure 2.4: (A) CryoTEM image of Aβ42 fibrils. Inset shows CPK model of 9 planes of a filament, one plane consisting of two monomers, prepared using PDB file 5KK3 [62] in PyMol [68]. The fibril shows presence of positively charged residues (blue), negatively charged residues (red), and hydrophobic residues (yellow), exposed on the fibril surface. (B) Solid-state NMR structure of Aβ42 fibril [62].

2.3 Driving Forces in Protein Self Assembly

The major driving force of protein folding is the hydrophobic effect. On top of this, electrostatic interactions also play a role in protein folding and stability. Aβ42 contains a large number of hydrophobic as well as charged amino acid residues, which can not only dictate the self-assembly process, but also influence the catalysis of monomer growth if they are exposed on the fibril surface.

2.3.1 Hydrophobic Effect

Certain molecules such as hydrocarbons are insoluble in water. This is known as the hydrophobic effect. In a protein sequence, certain amino acids such as valine, alanine, phenylalanine, or tyrosine have hydrophobic side chains. Proteins tend to fold in a way such that the non-polar surface that is exposed to water is minimal. As a result, there is a tendency for hydrophobic molecules to isolate themselves from contact with water, and during protein folding the hydrophobic side chains become buried in the interior of the protein [69]. This hydrophobic effect is a major force in protein folding [70, 71].

The sequence of Aβ42 consists of a large number of hydrophobic residues. Most of these are buried in the interior of the fibril core in the Aβ42 fibril structure, but there are some which are exposed on the surface and to the

solvent [62] (Figure 2.4 (B)). There are four such hydrophobic residues on the flexible N-terminal segment of Aβ42, and four on the fibril core. These residues on the fibril core, Val18, Ala21, Val40, and Ala42, are located in such a way that they form two continuous hydrophobic strips on each filament in the fibril. The effects of these particular hydrophobic residues at the N-terminal part and on the fibril core on the aggregation behavior of Aβ42 are investigated in **Paper I** and **Paper II** in this thesis.

2.3.2 Electrostatic Interactions

Certain amino acids such as aspartic acid, glutamatic acid, arginine, lysine, and histidine have ionizable side chains. The charges on these amino acids can be modulated by altering the pH of the solvent [72]. This can cause significant effects on the behavior of the protein. Since charged residues can be positive or negative, they can give rise to attractive or repulsive forces with respect to protein folding. Thus, interactions between charged residues can confer specificity [73]. These residues also impart a net charge to the protein, which can have significant implications on protein solubility and interactions.

The sequence of Aβ42 consists of a number of charged residues, and the net charge of Aβ42 is negative. This can affect on the interactions of Aβ42 with other biomolecules such as membranes, which also possess a net negative charge. The charged residues of Aβ42 are not studied in this thesis, but their role in the aggregation behavior of the peptide will be touched upon in more detail in Chapter 5.

3 Methods

"Science is like a love affair with nature; an elusive, tantalising mistress. It has all the turbulence, twists and turns of romantic love, but that's part of the game."

- *Vilanayur S. Ramachandran*

3.1 Chromatographic methods for purification

The importance of purity of sample can not be overstated while working with the Aβ peptide. Minor traces of impurity can perturb the aggregation kinetics and make it difficult to get reproducible behavior. To ensure the sequence purity of the peptide, we express the peptide recombinantly. To remove all possible contaminants, we perform ion exchange chromatography followed by multiple rounds of size exclusion chromatography.

3.1.1 Ion Exchange Chromatography

Ion exchange chromatography (IEC) separates proteins on the basis of their net charge. The stationary phase in IEC consists of tiny beads, usually called a resin, to which chemicals possessing a charge are attached. In cation exchange chromatography, negatively charged groups are attached to the beads, and they bind to positively charged compounds in the mobile phase. While in anion exchange chromatography, positively charged groups are attached to the beads, and they bind to negatively charged compounds in the mobile phase. The protein bound to the beads is then eluted by stepwise changing the mobile phase pH or salt concentration, which affects the net charge of adsorbed protein [74].

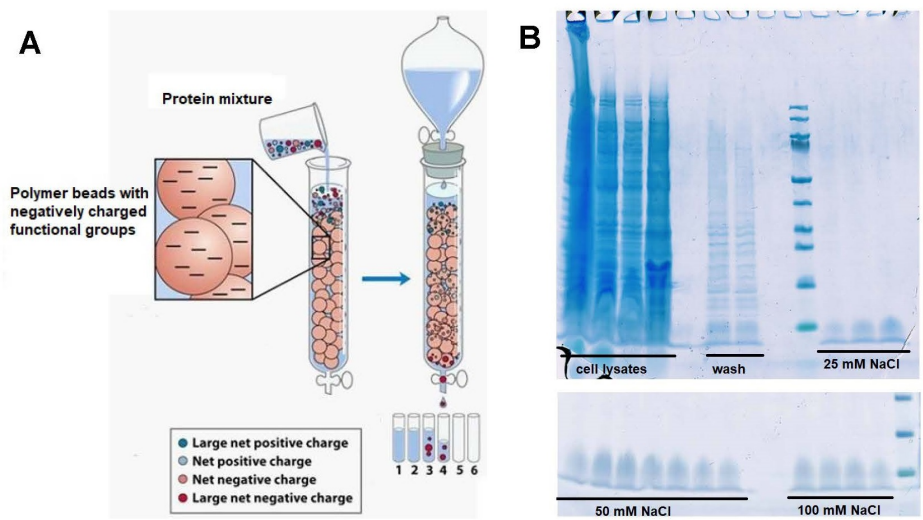

Figure 3.1: (A) Schematic representation of cation exchange chromatography [75]. (B) SDS-PAGE gel from anion exchange purification of a mutant form of Aβ42 studied in this thesis. Increasing salt concentration promotes the peptide to elute from the resin.

3.1.2 Size Exclusion Chromatography

Size Exclusion Chromatography (SEC), also known as gel filtration chromatography, separates proteins on the basis of their size [76]. The stationary phase in SEC is a gel composed of spherical porous beads. When the protein sample is passed through in the mobile phase as an aqueous flow, proteins of different sizes interact differently with the pores in the stationary phase. Proteins of smaller size are retained in the pores and stay longer in the stationary phase before eluting, while larger proteins will elute more rapidly as they will not be retained within the pores. Thus, the elution time of the protein is dependent on its size. While working with Aβ42, it is highly desirable to purify fresh monomers using SEC before setting up any experiments, to ensure the monomeric nature of starting material, and to remove all impurities in order to avoid perturbation of aggregation kinetics, which are sensitive to these.

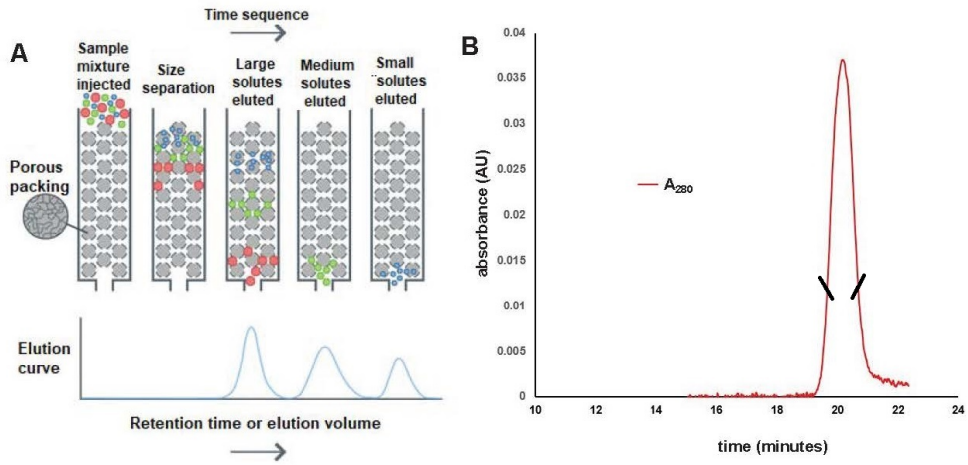

Figure 3.2: (A) Schematic representation of size exclusion chromatography (B) a typical SEC chromatogram showing elution peak for Aβ42 monomers from a 26x600 mm Superdex 75 column. The sample collected from the middle part of the peak is used for further experiments.

3.2 Thioflavin T

Thioflavin T (ThT) is a fluorescent dye that has become ubiquitously associated with work in the amyloid field. ThT gives strong fluorescence upon binding to amyloids and helps follow the aggregation process of amyloid proteins. The ThT molecule has a benzyl ring and a benzothiazole ring connected by a single carbon-carbon bond. In solution, these rings rotate

freely around this bond and as a result, the quantum yield is low. However, when ThT binds to amyloid structures, the rotation of these rings stops as they are locked, increasing the quantum yield. In the presence of amyloids, ThT has an excitation maximum at 450 nm, and an emission maximum at 482 nm wavelength [77]. When the dye concentration is optimized carefully, the fluorescence signal is linearly related to fibril mass concentration, which means that kinetic analysis of ThT fluorescence assays have also helped understand the microscopic steps involved in the mechanism of Aβ42 aggregation [42].

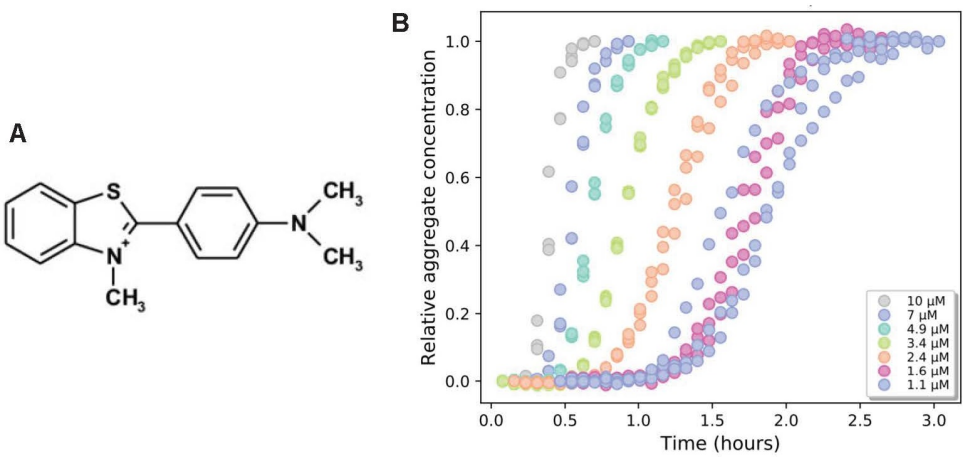

Figure 3.3: (A) Molecular structure of Thioflavin T. (B) a typical ThT fluorescence assay for a concentration range of Aβ42.

3.3 Cryogenic Electron Microscopy

Cryogenic Electron Microscopy (cryoEM) is a fast-evolving and increasingly used technique in the field of structural biology. The number of structures reported from single particle analysis (SPA) using cryoEM is increasing exponentially [78, 79]. CryoEM has been extensively used in this thesis as a characterization technique for fibril morphology of Aβ42 and its mutants. As the name suggests, electron microscopy uses a beam of electrons emitted from an electron gun to image biological macromolecules. Electrons are scattered by molecules in the air, and so electron microscopes must be operated in a high vacuum. For this reason, an electron microscope setup is equipped with a series of vacuum pumps. Thus, the samples are imaged under a high vacuum and at liquid nitrogen temperatures.

The EM column consists of three lens systems. Each lens system has its own lens, deflectors, stigmators, and apertures. The deflectors and stigmators aid the lens in focusing the electron beam on the sample and onwards to the detector. Apertures block the electrons that are going far from the optical axis of the lens, because these cause blurring of the image. The detector then helps create high-resolution images from the electrons emerging from the sample [80].

3.3.1 Plunge Freezing

The plunge freezing method of sample preparation has helped accelerate the cryoEM revolution. Developed by Jacques Dubochet, which won him the Nobel prize in Chemistry in 2017, this method helps preserve the sample in its near-native state for imaging [81]. A very small amount of sample is placed on an EM grid, suspended above a reservoir of liquid ethane. The liquid ethane is cooled by liquid nitrogen, maintained at -184 ^{o}C. After the sample is applied onto the grid, the grid is pressed against a pad of filter paper, absorbing most of the material. This is then rapidly plunged into liquid ethane. If the sample is thin enough, the heat is transferred into the liquid ethane so quickly that the water molecules don't have time to form ice crystals.

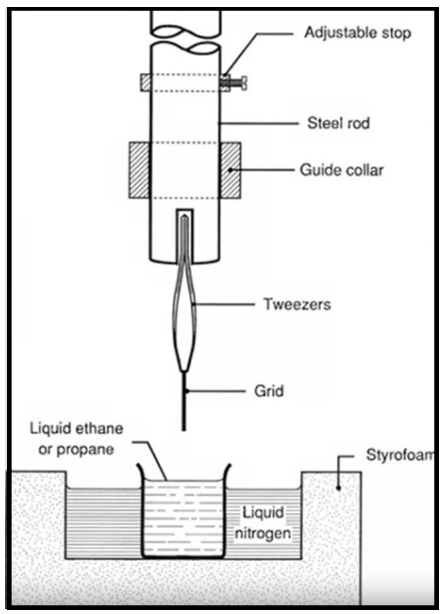

Figure 3.4: Schematic representation of a plunge freezing setup.

3.4 Direct Stochastic Optical Reconstruction Microscopy

In this thesis, we have used Direct Stochastic Optical Reconstruction Microscopy (dSTORM) to image peptides with covalently labelled fluorophores. dSTORM is a super-resolution microscopy technique that operates fluorophores as photoswitches and provides an optical resolution of 20 nm [82]. These photoswitches are able to be reversibly cycled between a fluorescent and dark condition by irradiation. This method of microscopy involves imaging the fluorophore-labelled molecules individually over a period of time, allowing the position of thousands of molecules to be determined, and uses this information to create a high-resolution image [83]. dSTORM can be used to image tissue sections as well as proteins *in vitro*. Another advantage of dSTORM is that it is relatively simple and cheap to set up. Two or more imaging channels are possible in dSTORM, which means that interaction between two different types of biomolecules can be studied by labelling them with different fluorophores.

We use dSTORM in **Paper III** and **Paper IV** of this thesis, with the help of our collaborators *M. Barghouth* and *E. Zhang*.

4

Discussion of Papers

"The great tragedy of science - the slaying of a beautiful hypothesis by an ugly fact."

- Thomas Huxley

4.1 Paper I

The idea for this project was born after the solid-state NMR structure of the Aβ42 fibril core was resolved [62]. Exposed on the fibril core of the Aβ42 fibril surface are four hydrophobic residues - Val18, Ala21, Val40, and Ala42. These four residues are arranged in such a way that they form two hydrophobic patches - Val18 and Ala21 forming one patch, and Val40 and Ala42 forming the other. Each filament cross-section of Aβ42 consists of two monomers, and hence these two hydrophobic patches are found twice in each cross-section. Hence, along the length of a filament, Val40 and Ala42 form a continuous hydrophobic strip. Val18 and Ala21 are located in a continuous hydrophobic groove along the filament length. Since secondary nucleation is associated with a low energy barrier of entropic nature [84], it seemed reasonable to expect that the exposed hydrophobic surfaces on the fibril core might play a role in the binding of monomers and their subsequent catalysis towards nucleation on the fibril surface. To test this hypothesis, we created seven serine substitution mutants - four single mutants for each hydrophobic residue; two double mutants for each hydrophobic patch (18+21) and (40+42); and a quadruple mutant to replace all hydrophobic residues with the hydrophilic serine.

Aggregation kinetics performed as a function of time and concentration showed that for all these seven serine mutants, while the lag phase of aggregation was somewhat extended, the serine substitution did not have a significant effect on secondary nucleation, as all of them still showed secondary nucleation as the dominant nucleation route in their aggregation process. A surprising result was however seen in the cross-seeding studies, which are performed for each mutant with *wild type* (WT) Aβ42 to probe whether the WT monomers are catalyzed on the surface of mutant fibrils, and *vice versa*. Under normal circumstances, the aggregation of monomers is catalyzed by the presence of seeds, which can be noticed by the shortening of the lag phase with increasing concentration of seeds. This seeding effect was however missing in the case of V18S, as WT monomers failed to catalyze on V18S seeds. This effect was also missing in the other mutants containing the V18S substitution, namely the double mutant (18+21)S, and the quadruple mutant 4S (figure 4.1).

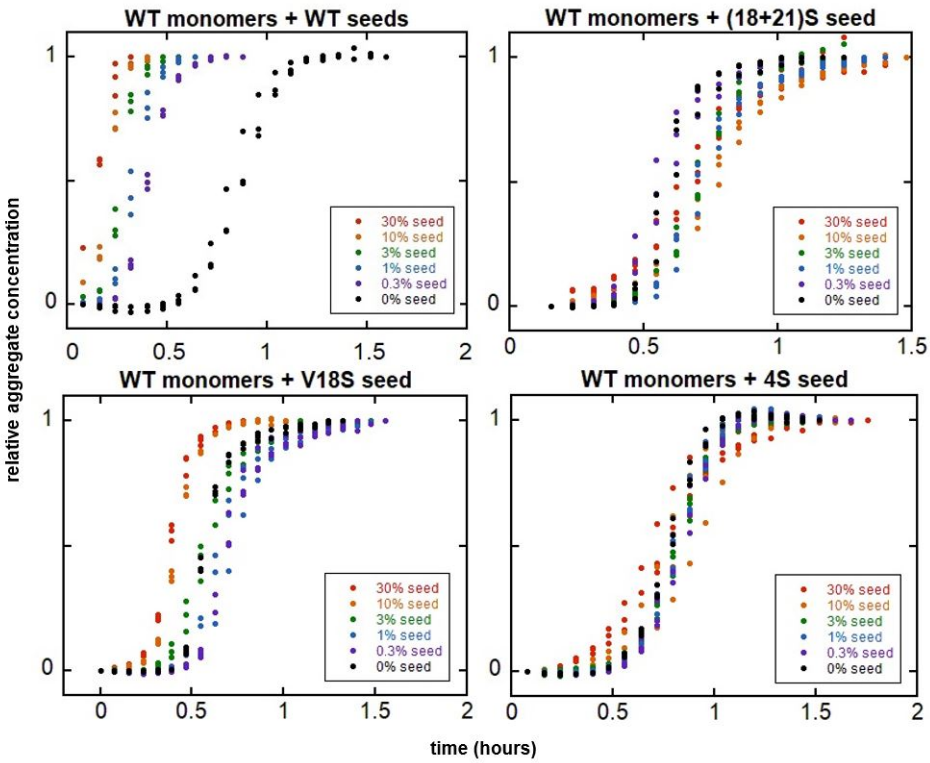

Figure 4.1: Cross-seeding aggregation kinetics of mutants containing V18S substitution with WT Aβ42. Self-seeding of WT monomers with WT seeds is shown in comparison. A clear shortening of the lag phase can be seen with increasing seed concentration. However, this effect can not be observed for WT monomers with seeds of V18S, (18+21)S, and 4S.

To get a better idea of what could be different about these fibrils which fail to catalyze WT monomers, we performed cryoTEM imaging to study fibril morphology. An interesting result was seen here as well. All the fibrils which failed to catalyze nucleation of the WT monomers were observed to show markedly different morphology as compared to WT fibrils. These fibrils have much longer distances between the "nodes" which are observed in a typical fibril by the two filaments twisting over each other. On the other hand, the other mutants which were capable of catalyzing WT monomers, namely A21S, V40S, A42S, and (40+42)S, showed morphology similar to WT fibrils, with shorter distances between nodes. In fact, measuring the node-to-node distances in these fibrils, which can be used as a proxy for fibril morphology, helped us classify the seven serine mutants into two different groups - peptides containing the V18S mutation in one morphology group (group B), and the remaining in the other (group A).

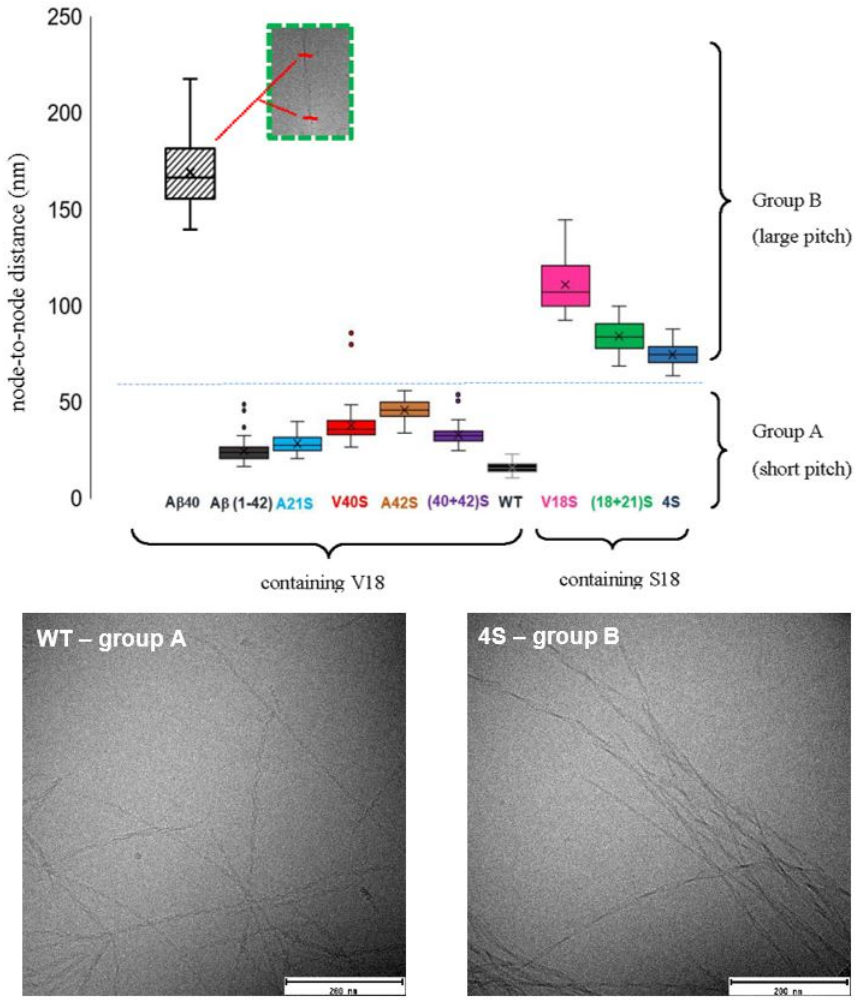

Figure 4.2: Analysis of fibril morphology based on cryoTEM images leads to the classification of serine mutants into two groups. Mutants of group B form fibrils that cannot catalyze the growth of monomers of group A peptides. Bottom panel shows cryoTEM images of fibrils of a peptide of each group; WT - belonging to group A, and 4S, belonging to group B

Since it is plausible that fibrils showing different morphology might have taken up a different fibril structure, we performed ANS fluorescence studies. ANS is a fluorescent probe that binds to hydrophobic surfaces and when excited at 350 nm, gives a fluorescence maximum at 490 nm, in contrast to 530 nm in water. We noticed strong ANS fluorescence in presence of 4S fibrils. In principle, 4S should not show ANS fluorescence since all four hydrophobic residues exposed on the fibril surface are replaced by serine. However, since it clearly has hydrophobic surfaces that bind ANS, this

indicates that the other hydrophobic residues in the Aβ42 sequence which are buried in the WT fibril core, are now exposed on the fibril surface due to the peptide folding differently and taking up a different fibril structure. This strongly points to the fact that fibril structure (or morphology) plays a big role for the monomer to be able to catalyze on the fibril surface.

Further seeding studies reveal that group B mutants show good cross-seeding with each other, but not with other serine mutants of group A. Additionally, Aβ40 fibrils are known to be unable to catalyze the growth of WT Aβ42 fibrils [85]. We noticed that Aβ40 fibrils have similar morphology to group B mutants, and seeding experiments also show good cross-seeding with group B Aβ42 mutants.

This paper hence shows the importance of fibril structure in surface catalyzed secondary nucleation, which is strongly linked with the ability of the monomers to take up the parent fibril structure. It will be interesting to get structural details on the fibrils of a mutant such as 4S, which would give us information on the surface exposed residues that make the growth of the WT monomers incompatible, and also more insight on how the V18S mutation switches fibril structure.

4.2 Paper II

This project was a logical follow-up to **Paper I**. While in **Paper I** we investigated the role of hydrophobic residues on the Aβ42 fibril core surface, in this project we focus on the hydrophobic residues at the flexible N-terminal part of Aβ42. There are four such residues at the N-terminal segment - Ala2, Phe4, Tyr10, and Val12. We create a series of mutants at these positions to decrease the hydrophobicity and test how this changes the aggregation behavior of the peptide. Additionally, we also include Y10F as a mutant with more hydrophobicity than WT Aβ42 at the respective position.

Aggregation kinetics were performed for all mutant peptides as a function of peptide concentration and time. This showed a clear role of hydrophobicity at these positions especially on primary nucleation, but also on the secondary nucleation. Figure 4.3 shows the comparison of aggregation curves for all variants followed at $\sim$5 μM monomer concentration.

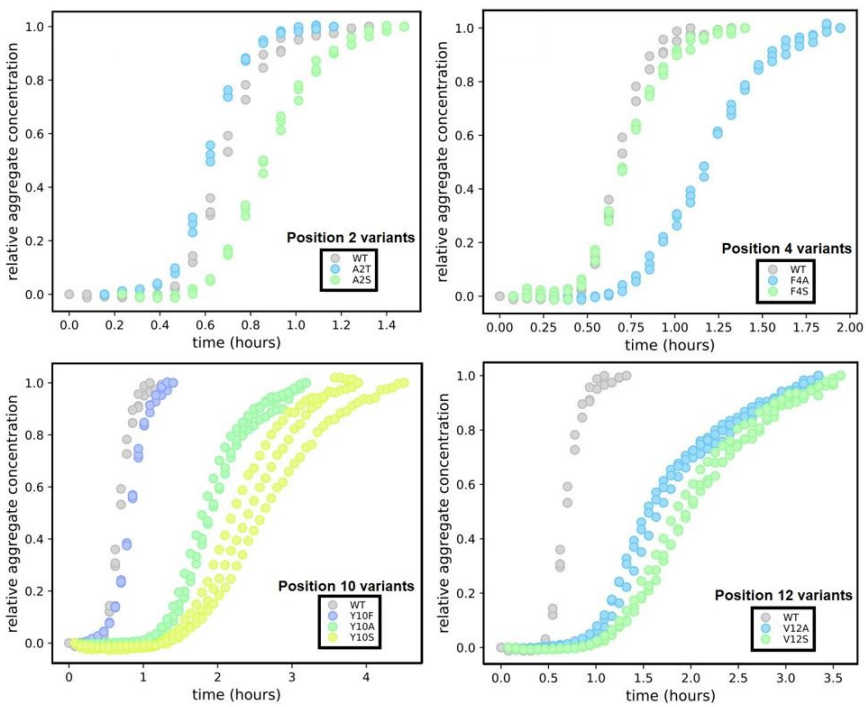

Figure 4.3: Aggregation curves for mutants created at different positions of the N-terminal segment of Aβ42 in comparison with WT. Aggregation curves are shown for representative monomer concentration close to 5 μM.

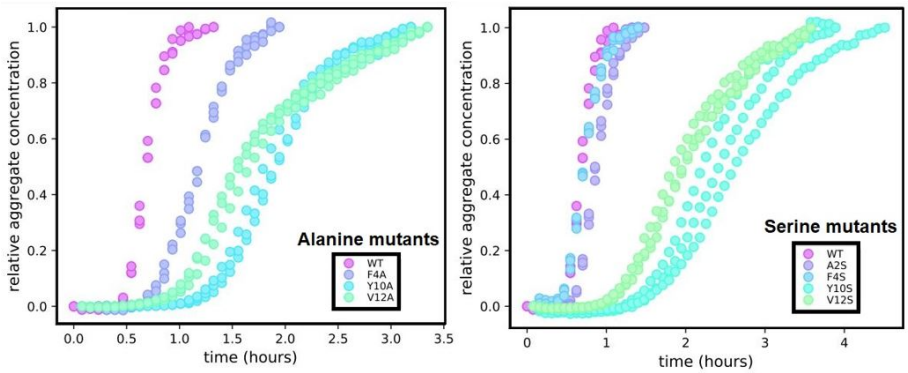

Figure 4.4: Comparison of aggregation curves for mutants involving Ala substitutions and Ser substitutions at positions 2, 4, 10, and 12, along with WT peptide. Aggregation curves are shown for representative monomer concentration close to 5 μM.

The most significant retardation of secondary nucleation is observed by replacing Tyr10 and Val12 with smaller hydrophobic (Ala) or hydrophilic (Ser) groups. This can be seen by the reduced steepness of the exponential phase in the aggregation curve. This effect is more prominent for Y10A and Y10S, which show reduced formation of fibril mass via secondary pathways by almost one order of magnitude. The Y10F mutation, which removes the polar nature of Tyr at position 10 only slightly hinders secondary nucleation. It is notable that Y10A, Y10S, V12A, and V12S mutations all cause an extended lag phase as well, in addition to affecting secondary nucleation.

An interesting observation is that the Ala substitution at position 4 (F4A) seems to hinder secondary nucleation more than the Ser substitution (F4S) (figure 4.3 and 4.4). However, it can be noted that while lowered hydrophobicity at the N-terminal region affects secondary nucleation, it still remains a dominant process in the aggregation mechanism of all the mutants because primary nucleation is even more retarded.

Cryo-TEM micrographs show that the mutants with lowered hydrophobicity appear to form significantly longer fibrils than WT. This can be attributed to the monomer being utilized more for elongation and fibril growth when secondary nucleation is affected. One such example is shown in figure 4.5 as a comparison between Y10F and Y10A.

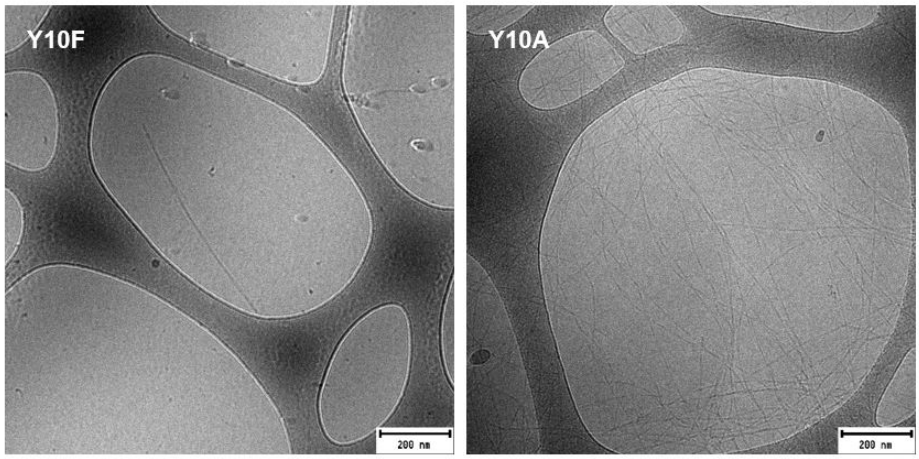

Figure 4.5: Fibrils formed by Y10F and Y10A reflect an inflated rate of elongation in order to accommodate monomer utilization due to lowered secondary nucleation. WT Aβ42 fibrils can be seen in figure 4.2 for comparison.

In **Paper I** we saw that secondary nucleation is a general feature whose presence is robust towards sequence perturbations. The findings of this project, and the dominance of secondary nucleation in the aggregation mechanism of all the studied mutants, support the idea of the generality and robustness of secondary nucleation. We also understand from this study, and previous papers, that while factors such as hydrophobicity play a role in secondary nucleation, it is not dependent on one particular feature of the peptide.

4.3 Paper III

Covalent labelling of fluorophores to biomolecules is highly desirable since it can open up a vast number of possibilities in terms of fluorescence-based single-molecule techniques available to us for gaining insight into the molecular mechanisms of events underlying the disease. This has proved to be challenging in the past with Aβ42 and has led to perturbations in aggregation kinetics and fibril morphology. This project is a small detour from the path of this thesis so far, but important for the next step in understanding secondary nucleation and other mechanistic studies of Aβ42 aggregation and cellular uptake. Since fluorophores typically have the size comparable to 7-10 amino acid residues and may be both hydrophobic and charged, careful consideration is required while labeling them to a small peptide such as Aβ42. In this study, we build on the information we have about residues in the Aβ42 sequence, particularly about their position in fibril structure and their role in peptide behavior through the mutants previously studied, and try to label fluorophores at various positions. We then tested these positions for the covalent attachment of the fluorophores and investigated which one of them causes the least perturbation of aggregation kinetics and fibril morphology.

In order to covalently attach the fluorophore, we introduce cysteine mutations at five different positions in Aβ42 and create the mutants S8C, Y10C, S26C, V40C, and A42C (figure 4.6). Covalent labelling is then performed using maleimide chemistry.

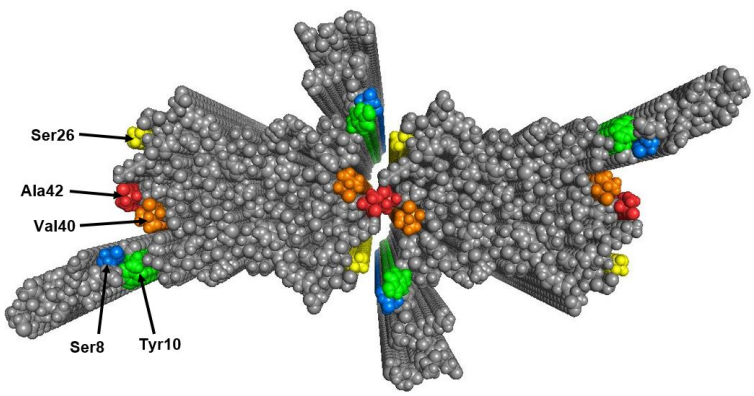

Figure 4.6: Structure of Aβ42 fibrils with four monomers per plane. The positions where cysteine is introduced through site directed mutagenesis are shown - Ser8 (blue), Tyr10 (green), Ser26 (yellow), Val40 (orange), Ala42 (red). These are the positions used for covalent attachment of Alexa fluorophores.

Out of these, Ser8 and Tyr10 are on the N-terminal part of Aβ42, which is flexible in the fibril structure. Ser26, Val40, and Ala42 are exposed on the surface of the fibril core in two monomers per plane of a fibril, and buried between two filaments of the fibril in the other two monomers per plane.

We successfully attach Alexa-fluor covalently to all the mutants. We find that the mutants with Alexa attached at the N-terminal segment, namely S8C and Y10C, are able to aggregate independently. When aggregating in the presence of unlabelled WT Aβ42, the aggregation kinetics do not show much perturbation for either S8C-Alexa or Y10C-Alexa. However, when aggregating independently, the lag phase for both these peptides is extended. Additionally, S8C-Alexa shows very similar fibril morphology to WT Aβ42 when aggregating in the presence of WT, but forms shorter fibrils independently. On the other hand, Y10C-Alexa fibril morphology seems greatly perturbed both with and without the presence of WT. We already saw in **Paper II** that mutations at the Tyr10 position cause changes in the aggregation profile. While Tyr10 is located on the unstructured N-terminal region of Aβ42, it is still very close to the fibril core. It makes sense that having a large molecule such as an Alexa fluorophore attached to this position greatly alters fibril structure as well.

S26C, V40C, and A42C require the presence of unlabelled WT monomers in order to form fibrils, when labelled with Alexa. In **Paper I** we saw that mutations at Val40 and Ala42 do not affect aggregation kinetics and fibril morphology. In line with this, attaching Alexa fluor to V40C and A42C does not cause significant perturbations in aggregation kinetics and fibril morphology. However, S26C serves as an example of how fluorophore labelling can greatly perturb aggregation kinetics and fibril morphology. As can be seen in figure 4.5, two monomers in each plane of the fibril are positioned in a way that their 26th residues face each other where the two filaments meet. Having a large moiety such as Alexa positioned here is sterically impossible and can be expected to greatly alter fibril structure.

Figure 4.7 compares S8C-Alexa488 and S26C-Alexa647 in terms of aggregation kinetics and fibril morphology, and gives an example of low perturbation in contrast to high perturbation.

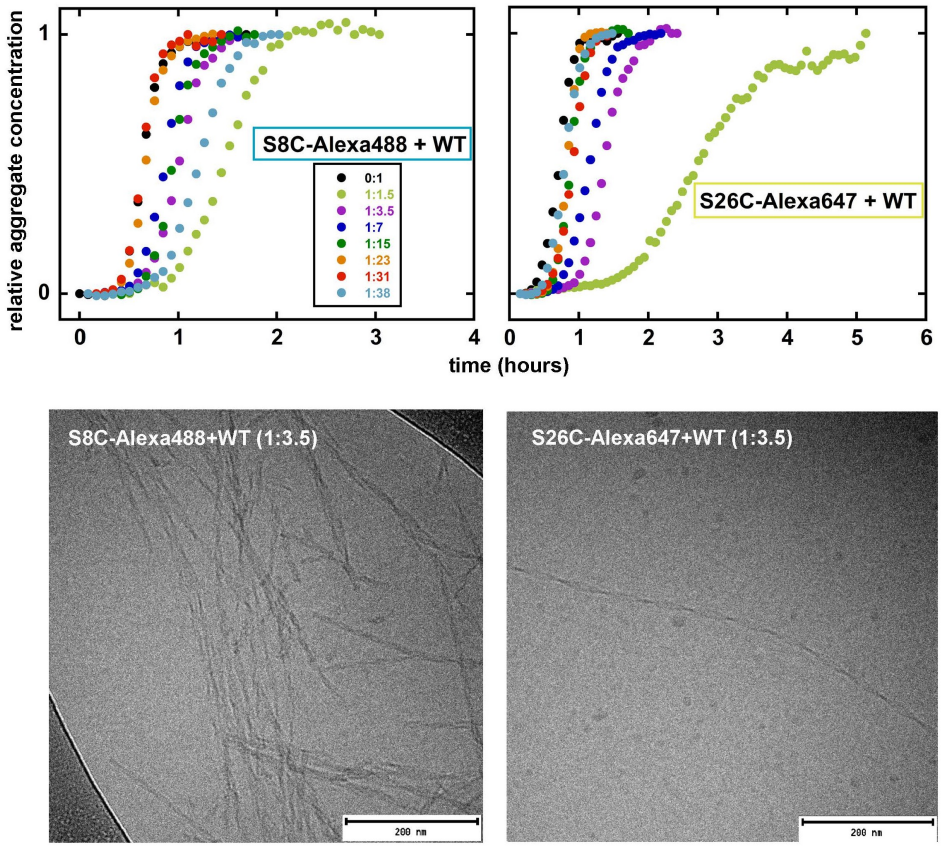

Figure 4.7: Aggregation kinetics for Alexa-labelled peptides S8C and S26C in presence of different ratios of WT Aβ42. The total monomer concentration is 5 μM and the curves represent median value of three replicates for each ratio. We can see an extended lag phase with S26C, which increases with increasing ratio of labelled peptide. The color code is the same for both peptides. Below, fibril morphology as studied by cryoTEM. S26C fibrils are elongated, and show longer node-to-node distances, which we used as proxy for fibril morphology in **Paper I**.

We can also say with confidence that while the molecular structures of Alexa488 and Alexa647 are very different, this does not seem to effect fibril formation or fibril morphology, which we tested by comparing V40C-Alexa488 and V40C-Alexa647 (figure 4.8).

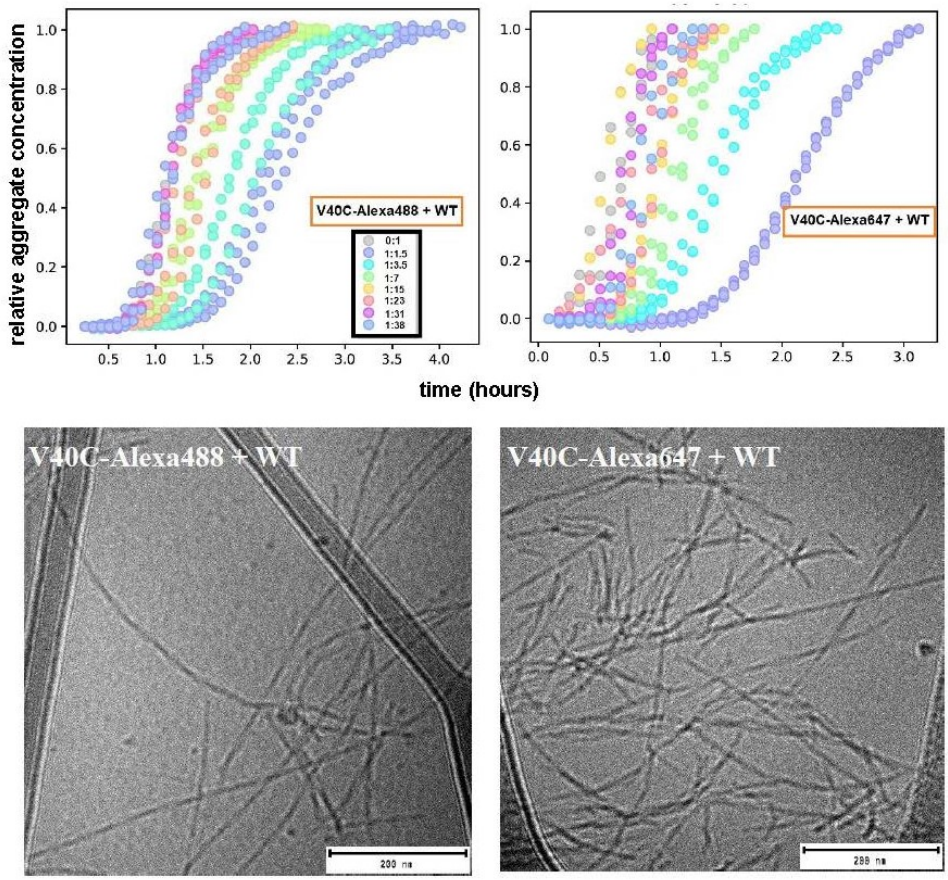

Figure 4.8: Aggregation kinetics of V40C-Alexa488 and V40C-Alexa647 in presence of different ratios of WT Aβ42. The total monomer concentration is close to 5 μM. V40C-Alexa488 and V40C-Alexa647 show similar profile and time scale of aggregation, proving that both Alexa488 and Alexa647 have the same effect of low perturbation on aggregation of the peptide. Color codes given in the left panel are the same for all both the peptides. The bottom panel shows cryoTEM images of end-stage fibrils of V40C-Alexa488 and V40C-Alexa647 in presence of 1:3.5 WT Aβ42. V40C-Alexa488 and V40C-Alexa647 show similar profile fibril morphology, proving that both Alexa488 and Alexa647 have the same effect of low perturbation on fibril morphology.

In conclusion, we successfully label these peptides with Alexa-fluors. These peptides form fibrils that can be detected in fluorescence-based microscopy techniques such as dSTORM (figure 4.9).

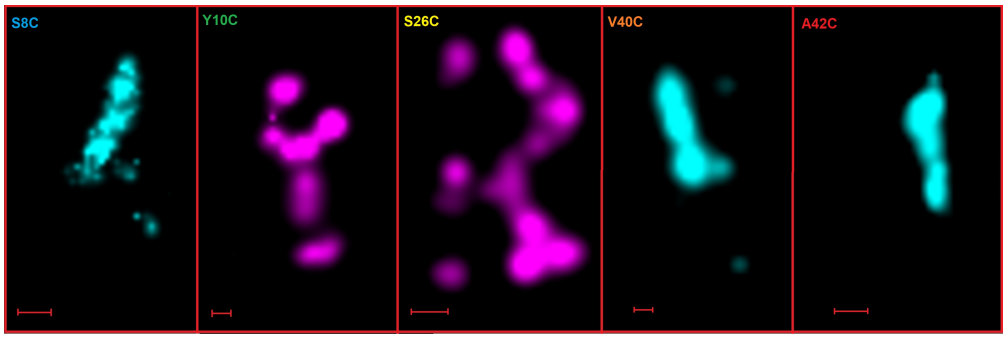

Figure 4.9: dSTORM images of end-stage fibrils of Alexa-labelled peptides S8C-Alexa488, Y10C-Alexa647, S26C-Alexa647+WT(1:3.5), V40C-Alexa488+WT(1:3.5), A42C-Alexa488+WT(1:3.5). The scale bar represents 200 nm.

4.4 Paper IV

Equipped with the fluorophore-labelled mutant Aβ42 peptides from **Paper III**, in this project we set out the answer some more questions about secondary nucleation. The main aim here is to perform dSTORM imaging of surface-catalysis of monomers on pre-formed fibrils along various time points of the aggregation reaction in order to study the nature of the interaction between monomers and fibrils. We choose S8C as a model for WT Aβ42 in this project because, as we saw, it can aggregate independently, and it shows insignificant perturbations on aggregation kinetics and fibril morphology when labelled with Alexa-fluor. Additionally, we also include the 4S mutant from **Paper I**. We saw that this mutant includes four total substitutions - V18S + A21S + V40S + A42S, and the fibrils formed by this mutant Aβ42 do not catalyze the aggregation of WT Aβ42. By performing dSTORM imaging of the cross-seeding reaction between WT monomers and 4S fibrils, and comparing it with the self-seeding of WT, we can gain insight into what goes on during the surface-catalyzed secondary nucleation process.

In order to covalently attach Alexa-fluor to the 4S peptide, we need to introduce a cysteine residue in the sequence so that we can use maleimide chemistry for the labelling. As we saw in **Paper III**, S8C mutants independently form very short fibrils, and so it might not be an appropriate labelling position for the 4S mutant, as the non-catalytic behavior of 4S fibrils towards WT monomers is highly dependent on fibril morphology and structure. Since a V40C mutation causes insignificant perturbations on fibril morphology, we choose to introduce this cysteine at residue 40. We are also preserving the V18S substitution of the 4S mutant, which as we saw in **Paper I**, is the key in causing the structural switch of the mutant fibrils. Thus, the 4S mutant is now a combination of the substitutions - V18S + A21S + *V40C* + A42S.

In order to visualize the difference between the two interacting entities, we must also have monomers and fibrils labelled with different fluorophores. We select Alexa488-labelled monomers to form the "seeds" and Alexa647 to label the monomeric species. To perform seeding studies using dSTORM, we first immobilize fibrils on a poly-L-lysine coated glass-bottom dish. The positively charged lysine helps the negatively charged Aβ fibrils bind to the surface. The reaction is then started by adding monomers in solution to the glass-bottom dish. At the end of each time point, the unbound monomers are washed away. Since the monomers are the reacting species, washing

the excess monomers away will stop the reaction. The glass-bottom dish is then used for imaging at the particular time point of reaction.

For the self-seeding reaction, we performed dSTORM every ten minutes, starting from t=10 mins to t=80 mins. At the early time-points of 10 and 20 mins, we see small clusters of monomers at fibril surfaces. As the reaction time progresses, a lot more of these monomer clusters can be noticed at fibril surfaces where they grow into larger aggregates covering the entire length of the fibril in some cases. When these aggregates keep growing, at a certain point they detach from the fibrils and can be found in solution as independent fibrils, which can then catalyze the growth of new monomers. Since the newly formed fibrils detach from the ones immobilized on the poly-L-lysine, only a few of these are observed bound to the poly-L-lysine on the glass surface. Most of the detached aggregates would be removed when the excess monomers are washed at the end of each time point. In the self-seeding reaction, we observe the auto-catalytic nature of Aβ42 proliferation. It is notable that monomer interaction and growth happens along the fibril surfaces (Figure 4.10). It can thus be said that secondary nucleation occurs along the entire length of the fibril, and involves the conversion of monomers into larger aggregates, which then detach from the parent fibril as individual fibrils in solution.

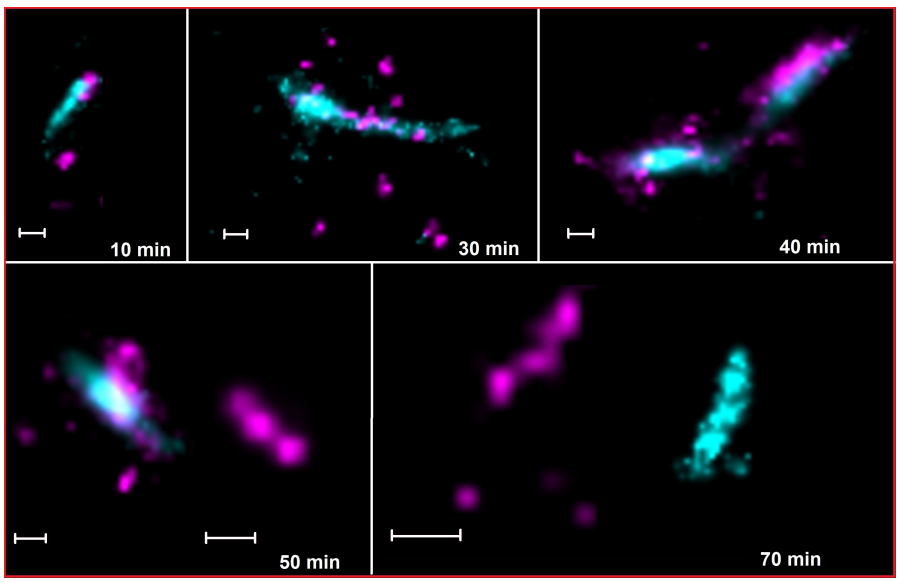

Figure 4.10: Highlights from the self-seeded aggregation studies to follow surface catalysis of WT Aβ42 on WT Aβ42 fibrils studied using dSTORM imaging. The aggregation reaction was followed using time points at 10 minute intervals. WT monomers are labelled with Alexa647 (fuchsia) and WT fibrils are labelled with Alexa488 (cyan). The scale bars represent 200 nm.

However, in the cross-seeding reaction, while monomers interact along fibril surfaces, we fail to detect growth on the surface. The only monomer growth occurs at the ends of the fibrils, *i.e.*, elongation (Figure 4.11). Apart from the failure of detecting growth at fibril surfaces, the other notable difference in the cross-seeding reaction is the time scale of the reaction. When the fibrils are catalytic to the monomers (substrate), the reaction progresses much faster and the end stage is observed ∼80 minutes in the self-seeding reaction. But without the catalytic nature of the fibrils, the cross-seeding reaction proceeds more slowly. The time points here are taken one hour apart, and the reaction is followed up to 5 hours to monitor elongation. It is only at very late time points (12 hours) that we see fibrils formed from the Alexa647 labelled monomers, presumably formed due to nucleation of the monomers that don't elongate on the seeds.

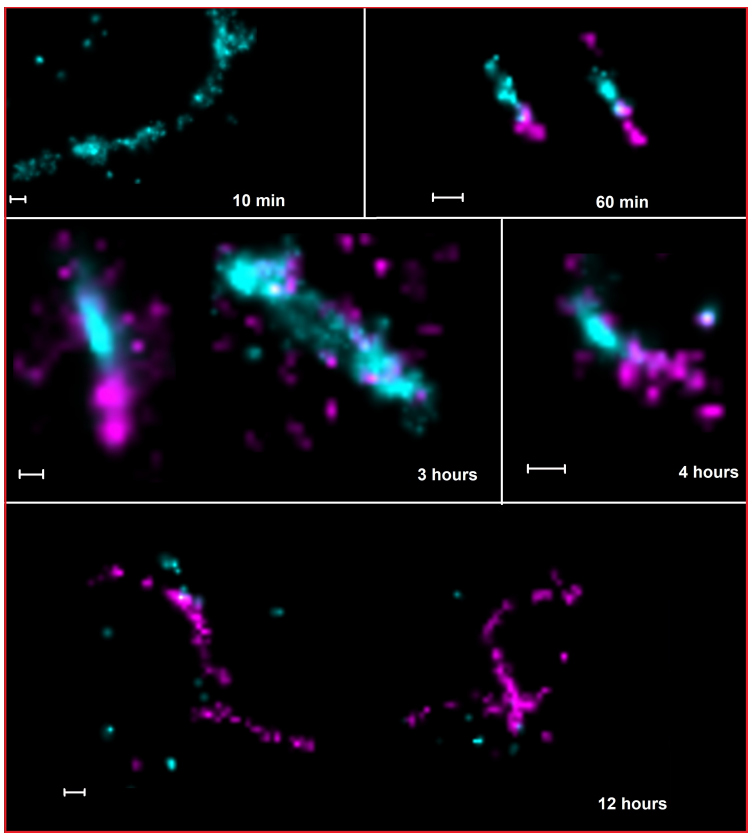

Figure 4.11: Highlights from the cross-seeded aggregation studies to follow surface catalysis of WT Aβ42 on 4S fibrils studied using dSTORM imaging. The aggregation reaction was followed using time points at 60 minute intervals. WT monomers are labelled with Alexa647 (fuchsia) and 4S fibrils are labelled with Alexa488 (cyan). The scale bars represent 200 nm.

Figure 4.12 summarizes the trend of monomer growth on fibrils in the self- and cross-seeding reactions. When surface catalyzed secondary nucleation drives the aggregation process, a clear exponential period of growth is noticed after an initial lag phase. After the aggregates have grown on the fibril surface, they start detaching from the fibrils and exist as independent fibrils in solution, and the original seeds are free from these aggregate species growing on them (figure 4.12(A)). However in the case of 4S fibrils, the WT monomers are only able to elongate the fibrils, and are unable to grow on their surfaces. As a result, growth from monomers is linear (figure 4.12(B)), as the time scale of elongation is slower than secondary nucleation. These monomers elongating on fibrillar ends remain a part of the original seeds, and do not detach as independent fibrils in solution.

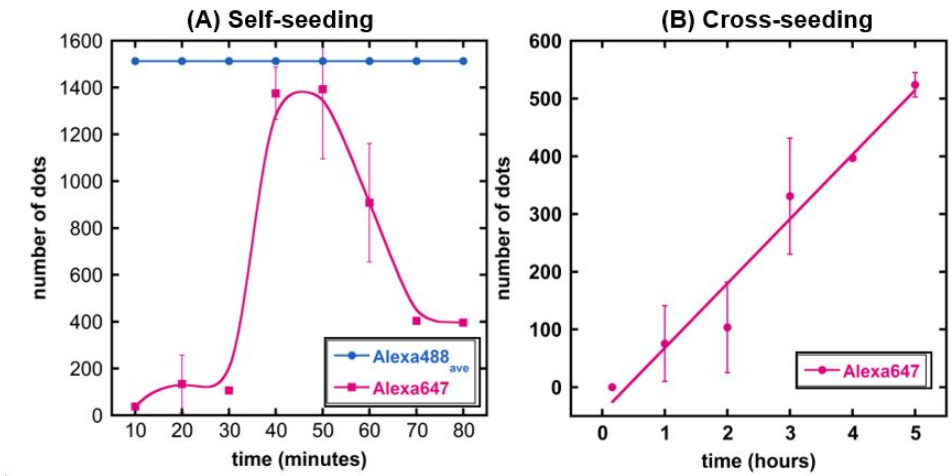

Figure 4.12: Comparison of monomer growth in the self- and cross-seeded aggregation. The semi-quantitative analysis is performed by counting small dots from Alexa488 (seeds) and Alexa647 (monomers) using ImageJ software. Each dot can be counted as one molecule. Error bars represent the standard deviation of Alexa647 signal from different image frames at each time point.

5

A brief review of what we know about secondary nucleation

"I did it for me. I liked it. I was good at it. And, I was really... I was alive."

- *Walter White*, Breaking Bad.

Secondary nucleation for proteins was first reported in 1985 for sickle cell haemoglobin [86]. Since then, it has been established as the dominant mechanism for the aggregation of other amyloid proteins such as IAPP [54], insulin [87], and α-synuclein [53, 88]. For Aβ42, it was in 2013 that the model for secondary nucleation dominated aggregation was established [42]. In this chapter, I will try to summarize what we know about secondary nucleation in Aβ42 so far, and what the findings in this thesis add to that information. Past evidence suggests that secondary nucleation does not depend on one particular part of the peptide sequence or fibril structure. Here, I will try to discuss the roles of the two different parts of the fibril structure in secondary nucleation, and other factors that affect it. While we will touch upon only the intrinsic factors affecting protein aggregation, it is worth keeping in mind that extrinsic factors such as pH [52], ionic strength [89], and temperature [84] are also known to affect secondary nucleation.

5.1 The role of the N-terminal region in secondary nucleation

As mentioned earlier, Aβ42 is generated by the cleavage of a larger transmembrane protein, APP, when APP is cleaved by β-secretase before Asp1 of the Aβ-domain [7]. However, there is now ample evidence that APP may be proteolyzed at residues other than at the canonical β-secretase site, and that Aβ exists as various length variants including both extensions and truncations at the N- and the C- terminus [90–93]. Six such extensions of 5 to 40 amino acids in length were studied, and it was observed that extensions at the N-terminus affect the rate constants of all microscopic steps involved in Aβ aggregation, including secondary nucleation. It also showed that the longer the extension, the larger the effect on the rate constants [94]. Interestingly, a truncated version of the peptide, Aβ5-42, was shown to be more prone to aggregation and have an enhanced rate of nucleation [95]. N-terminally truncated pyroglutamate-Aβ3-42 is also known to show increased aggregation propensity and increased neurotoxicity [96]. Simulation studies have also demonstrated that extensions at the N-terminus show retarded fibril formation due to the decreased probability of "productive" molecular encounters between monomers and fibrils [94]. It can thus be argued that the length of the flexible N-terminal segment that decorates the fibrils plays a role in secondary nucleation by influencing the interaction of monomers with the fibrils.

Recent studies have also investigated the role of the N-terminal segment amino acid sequence in secondary nucleation, where the order of the amino acids was scrambled, keeping the same composition in order to not affect the hydrophobicity or net charge. This also resulted in retardation of primary and secondary nucleation [97]. A high fraction of familial AD mutants, both pathogenic and protective, have been found in the N-terminal region. Other designed mutants which change the hydrophobicity or net charge have also been studied.

Two familial mutations are found at Ala2 position of Aβ42. One mutation - A2V, is pathogenic [98]. A2V increases the hydrophobicity of the peptide and shows an increased rate of secondary nucleation [52]. The second mutation - A2T, is protective [99]. A2T decreases the hydrophobicity of the peptide and lowers the rate of secondary nucleation and oligomer formation [100]. In **Paper II** we saw that mutants designed to alter hydrophobicity at various other positions in the N-terminal region also show an effect on the fibril mass produced via secondary nucleation.

At position His6, the familial mutant H6R is found to alter the net charge of the peptide by making it less negative [101]. H6R produces more oligomers, and these oligomers are more toxic to neuronal cells than wild type Aβ42 [102]. Two familial mutations are found at Asp7 position of Aβ42. The first mutation - D7N, removes a negative charge and adds a polar residue [103]. D7N causes increased production of oligomers and higher toxicity to neuronal cells [102]. The second mutation - D7H, removes a negative charge and adds a positive charge [104]. Histidine also affects the metal ion-binding properties of Aβ42, which are known to affect aggregation behavior. D7H is susceptible to the formation of ion-induced oligomers and exhibits greater toxicity [104]. Other mutants designed to alter net charge at the N-terminal part of Aβ40 have also shown an effect on various microscopic steps of the aggregation process [105].

So far, with regards to the N-terminal segment, we have touched upon extensions, truncations, amino acid sequence, hydrophobicity, and net charge, which all seem to affect secondary nucleation. While some of these factors lower the rate of secondary nucleation, none of them completely eliminate it, and it is still the main driving force of the aggregation process.

5.2 The role of the fibril core in secondary nucleation

The Aβ42 sequence contains a large number of hydrophobic residues. Most of these are buried in the fibril core, but four hydrophobic residues are exposed on the surface of the fibril core - Val18, Ala21, Val40, and Ala42 (figure 2.3) [62]. These four hydrophobic residues form two extended hydrophobic patches along the fibril surface. In **Paper I**, we saw that replacing these four hydrophobic residues with the hydrophilic serine does not eliminate secondary nucleation. Certain familial mutations are also found at these hydrophobic positions. A21G affects the hydrophobic side chain at residue 21 [106] and its degradation by proteolysis is significantly slower [107]. Some studies have shown that this mutation decreases the aggregation propensity of Aβ42 [108, 109]. Other studies show that A21G also has different fibril morphology as compared to WT Aβ42 [110].

Additional to the four exposed hydrophobic residues, the Aβ42 fibril core also has four charged residues exposed on the surface (figure 2.3) [62]. Two of these residues are positively charged - Lys16 and Lys28, and two residues are negatively charged - Glu22 and Asp23. A number of familial AD mutations are found at these positions. One mutation - E22Q [111], has one less negative charge than WT Aβ42. E22Q has nucleation rates about one order of magnitude higher than WT, but the secondary nucleus conversion rate is still comparable to WT. The fibrils of this peptide are relatively shorter than WT [110]. Another mutation - E22G [112], also has one less negative charge than WT but the size of the side chain is much smaller. Additionally, E22G mutation makes the peptide more hydrophobic. This significantly increases the aggregation propensity of E22G [110]. The nucleation rate constants are higher, and the fibrils formed by this mutant are shorter, pointing to an increased rate of secondary nucleation. E22G is also linked to a very aggressive early onset AD [113]. The third mutation at Glu22 - E22K [114], has two units less negative charge than WT, and replaces a negatively charged residue with a positively charged residue. E22K has significantly decreased secondary nucleus conversion rate, and distinctly changed fibril morphology [110]. At Asp23, the familial mutant linked to early onset AD is D23N [115]. This mutation conserves the size of the side chain but has one less negative charge than WT. D23N shows an enhanced aggregation rate and increased secondary nucleation rate constant [110].

An interesting familial mutation in the fibril core is the deletion mutation A$\beta42_{\Delta 19-24}$, which involves the deletion of six residues from the middle of

the peptide sequence [116]. Two of these six residues are Val18, and Ala21, which are exposed on the surfaces of the WT fibril, studied in **Paper I**. This mutant shows increased aggregation propensity compared to WT Aβ42, and is also known to form polymorphic fibrils.

Now, with regards to the surface of the fibril core, we have touched upon deletions, hydrophobicity, net charge, and size of side chains, which all seem to affect secondary nucleation. While some of these factors lower the rate of secondary nucleation, none of them completely eliminate it, and it is still the main driving force of the aggregation process. It is noteworthy however, that a common feature reported in a lot of these mutations is the resulting change in fibril morphology.

5.3 Specificity in secondary nucleation

While it is widely accepted that monomers growing at fibrillar ends via elongation take up the structure of the parent fibril, it is only very recently that the question has been asked if there is a similar templating role of the fibril structure involved in secondary nucleation.

The first indication of such a mechanism being involved was noticed during the cross-seeding studies of Aβ42 and Aβ40 [85]. Both these peptides are involved in the pathology of AD, and have the same peptide sequence, except for the two missing residues at the C-terminus of Aβ40. Yet, they are known to adapt different fibril structures. The morphology of the fibrils for both these peptides is markedly different [85]. The aggregation of Aβ42 monomers is not catalyzed by Aβ40 fibrils, and *vice versa*.

This idea of a templating role of secondary nucleation is perpetuated by the findings in **Paper I**, where we see that mutants with different fibril morphology, and likely a different fibril structure - namely V18S, (18+21)S, and 4S - fail to catalyze the aggregation of WT Aβ42 monomers. Here, we also saw that Aβ40, which fails to cross-seed with WT Aβ42, shows cross-seeding with these Aβ42 mutants. Indeed, these Aβ42 mutants have very similar fibril morphology to the Aβ40 fibrils. This presents a great starting point for further investigation, and obtaining the fibril structure of these mutants would provide useful information on the nature, characteristics, and features of the fibril surface which fails to catalyze monomers of the WT peptide in relation to the one that does.

Aβ37 and Aβ38 are other length variants of the Aβ peptide with trun-

cations at the C-terminus, that are physiologically abundant. A study following the interactions of Aβ37, Aβ38, Aβ40 and Aβ42 shows that both Aβ37 and Aβ38 show fibril morphology which is similar to Aβ40 fibrils [117]. Indeed, Aβ42 monomers do not cross-seed with Aβ37 and Aβ38 fibrils. However, Aβ40 monomers show cross-seeding with both these peptides to some extent [117]. This once again suggests a link between fibril morphology (or structure) and surface catalyzed secondary nucleation.

A recent study investigated the interaction between Aβ40 and Aβ16-22, another length variant that is involved in AD. Both seeded aggregation studies and molecular dynamic simulations were performed in this study. It was observed here that aggregation of Aβ40 monomers is catalyzed by Aβ16-22 fibrils. These monomers recognize structural features of fibrils and dock onto them, which catalyzes their assembly [118]. A similar phenomenon might be an explanation behind something noticed in **Paper IV**, where dSTORM experiments show that WT Aβ42 monomers do interact with the surface of 4S Aβ42 fibrils, but fail to grow into a larger nucleus on them. In contrast, the growth of monomer clusters into denser nuclei can be observed when WT Aβ42 monomers interact with WT fibrils. Could it be that there are specific sites on the fibril surface that are important for nucleation? Or perhaps growth by monomer nucleation requires structural compatibility?

Another recent study has shown that WT Aβ42 monomers fail to nucleate on the fibrils of a designed mutant S26Q, which seems to take up a different fibril structure [119].

Total Internal Reflection Fluorescence (TIRF) microscopy insights into secondary nucleation events have shown that fibrils formed by secondary nucleation resemble the parent fibril population, and that majority of the parent fibril population is capable of self-replication by secondary nucleation, rather than a small fraction of "superspreader" fibrils [120]. These studies also show that there is no correlation between secondary nucleation events and micrometer-scale morphological features such as the local curvature of fibrils. Further proof of the necessity of structural compatibility between monomer and parent fibril for successful seeding has come from studies showing the importance of chirality in the process of secondary nucleation [121]. These findings point to an underlying molecular mechanism involved in secondary nucleation.

On the whole, there seems to be growing evidence suggesting that the ability of monomers to nucleate on a fibril surface is indeed very strongly

linked to the ability of the monomers to take up the structure of the parent fibril.

References

[1] Rainulf A. Stelzmann, H. Norman Schnitzlein and F. Reed Murtagh. “An english translation of alzheimer’s 1907 paper, “über eine eigenartige erkankung der hirnrinde””. In: *Clinical Anatomy* (1995).

[2] Chengxuan Qiu, Miia Kivipelto and Eva von Strauss. “Epidemiology of Alzheimer’s disease: occurrence, determinants, and strategies toward intervention”. In: *Dialogues in Clinical Neuroscience* (2009).

[3] Jan Van Erum, Debby Van Dam and Peter Paul De Deyn. “Sleep and Alzheimer’s disease: A pivotal role for the suprachiasmatic nucleus”. In: *Sleep Medicine Reviews* (2018).

[4] C. L. Masters et al. “Amyloid plaque core protein in Alzheimer disease and Down syndrome”. In: *Proceedings of the National Academy of Sciences of the United States of America* (1985).

[5] Julie A. Schneider and David A. Bennett. “Where Vascular Meets Neurodegenerative Disease”. In: *Stroke* (2010).

[6] Sarah T. Pendlebury and Peter M. Rothwell. “Prevalence, incidence, and factors associated with pre-stroke and post-stroke dementia: a systematic review and meta-analysis”. In: *The Lancet. Neurology* (2009).

[7] Kaj Blennow, Mony J. de Leon and Henrik Zetterberg. “Alzheimer’s disease”. In: *The Lancet* (2006).

[8] L. Kilander et al. “The association between low diastolic blood pressure in middle age and cognitive function in old age. A population-based study”. In: *Age and Ageing* (2000).

[9] L. J. Launer et al. “Midlife blood pressure and dementia: the Honolulu-Asia aging study”. In: *Neurobiology of Aging* (2000).

[10] J. A. Luchsinger et al. “Diabetes mellitus and risk of Alzheimer’s disease and dementia with stroke in a multiethnic cohort”. In: *American Journal of Epidemiology* (2001).

[11] Rita Peila et al. “Type 2 diabetes, APOE gene, and the risk for dementia and related pathologies: The Honolulu-Asia Aging Study”. In: *Diabetes* (2002).

[12] Louis A. Profenno, Anton P. Porsteinsson and Stephen V. Faraone. “Meta-analysis of Alzheimer’s disease risk with obesity, diabetes, and related disorders”. In: *Biological Psychiatry* (2010).

[13] R. Doll et al. “Smoking and dementia in male British doctors: prospective study”. In: *BMJ (Clinical research ed.)* (2000).

[14] S. Koponen et al. “APOE-ε4 predicts dementia but not other psychiatric disorders after traumatic brain injury”. In: *Neurology* (2004).

[15] Chanung Wang and David M. Holtzman. “Bidirectional relationship between sleep and Alzheimer’s disease: role of amyloid, tau, and other factors”. In: *Neuropsychopharmacology* (2020).

[16] A. Bianchetti et al. “Predictors of mortality and institutionalization in Alzheimer disease patients 1 year after discharge from an Alzheimer dementia unit”. In: *Dementia (Basel, Switzerland)* (1995).

[17] B. Guarnieri et al. “Prevalence of sleep disturbances in mild cognitive impairment and dementing disorders: a multicenter Italian clinical cross-sectional study on 431 patients”. In: *Dementia and Geriatric Cognitive Disorders* (2012).

[18] L. Letenneur et al. “Are sex and educational level independent predictors of dementia and Alzheimer’s disease? Incidence data from the PAQUID project”. In: *Journal of Neurology, Neurosurgery, and Psychiatry* (1999).

[19] L. Letenneur et al. “Incidence of dementia and Alzheimer’s disease in elderly community residents of south-western France”. In: *International Journal of Epidemiology* (1994).

[20] D. A. Evans et al. “Education and other measures of socioeconomic status and risk of incident Alzheimer disease in a defined population of older persons”. In: *Archives of Neurology* (1997).

[21] D. A. Evans et al. “Level of education and change in cognitive function in a community population of older persons”. In: *Annals of Epidemiology* (1993).

[22] X. Zhang, C. Li and M. Zhang. “[Psychosocial risk factors of Alzheimer’s disease]”. In: *Zhonghua Yi Xue Za Zhi* (1999).

[23] Laura Fratiglioni, Stephanie Paillard-Borg and Bengt Winblad. “An active and socially integrated lifestyle in late life might protect against dementia”. In: *The Lancet. Neurology* (2004).

[24] N. Scarmeas et al. “Influence of leisure activity on the incidence of Alzheimer’s disease”. In: *Neurology* (2001).

[25] Nikolaos Scarmeas et al. “Mediterranean diet, Alzheimer disease, and vascular mediation”. In: *Archives of Neurology* (2006).

[26] Laura Jean Podewils et al. “Physical activity, APOE genotype, and dementia risk: findings from the Cardiovascular Health Cognition Study”. In: *American Journal of Epidemiology* (2005).

[27] G. G. Glenner and C. W. Wong. “Alzheimer’s disease: initial report of the purification and characterization of a novel cerebrovascular amyloid protein”. In: *Biochemical and Biophysical Research Communications* (1984).

[28] J. A. Hardy and G. A. Higgins. “Alzheimer’s disease: the amyloid cascade hypothesis”. In: *Science (New York, N.Y.)* (1992).

[29] Jie Kang et al. “The precursor of Alzheimer’s disease amyloid A4 protein resembles a cell-surface receptor”. In: *Nature* (1987).

[30] C. Bancher et al. “Accumulation of abnormally phosphorylated tau precedes the formation of neurofibrillary tangles in Alzheimer’s disease”. In: *Brain Research* (1989).

[31] M. D. Weingarten et al. “A protein factor essential for microtubule assembly”. In: *Proceedings of the National Academy of Sciences of the United States of America* (1975).

[32] M. P. Lambert et al. “Diffusible, nonfibrillar ligands derived from Aβ1–42 are potent central nervous system neurotoxins”. In: *Proceedings of the National Academy of Sciences* (1998).

[33] Roberta Ricciarelli and Ernesto Fedele. “The Amyloid Cascade Hypothesis in Alzheimer’s Disease: It’s Time to Change Our Mind”. In: *Current Neuropharmacology* (2017).

[34] Fuyuki Kametani and Masato Hasegawa. “Reconsideration of Amyloid Hypothesis and Tau Hypothesis in Alzheimer’s Disease”. In: *Frontiers in Neuroscience* (2018).

[35] Colin L. Masters et al. “Alzheimer’s disease”. In: *Nature Reviews. Disease Primers* (2015).

[36] Daniela Puzzo et al. “Behavioral assays with mouse models of Alzheimer’s disease: practical considerations and guidelines”. In: *Biochemical Pharmacology* (2014).

[37] Dominic M. Walsh and Dennis J. Selkoe. “A beta oligomers - a decade of discovery”. In: *Journal of Neurochemistry* (2007).

[38] Dennis J. Selkoe. “Alzheimer disease and aducanumab: adjusting our approach”. In: *Nature Reviews Neurology* (2019).

[39] Bart De Strooper. “Proteases and proteolysis in Alzheimer disease: a multifactorial view on the disease process”. In: *Physiological Reviews* (2010).

[40] Michael S. Wolfe. “Dysfunctional γ-secretase in familial Alzheimer’s disease”. In: *Neurochemical research* (2019).

[41] Erik Hellstrand et al. “Amyloid β-protein aggregation produces highly reproducible kinetic data and occurs by a two-phase process”. In: *ACS chemical neuroscience* (2010).

[42] Samuel I. A. Cohen et al. “Proliferation of amyloid-β42 aggregates occurs through a secondary nucleation mechanism”. In: *Proceedings of the National Academy of Sciences of the United States of America* (2013).

[43] Georg Meisl et al. “Molecular mechanisms of protein aggregation from global fitting of kinetic models”. In: *Nature Protocols* (2016).

[44] Paolo Arosio, Tuomas P. J. Knowles and Sara Linse. “On the lag phase in amyloid fibril formation”. In: *Physical Chemistry Chemical Physics* (2015).

[45] Alexander A Chernov. “Protein crystals and their growth”. In: *Journal of Structural Biology*. Macromolecular crystallization in the structural genomics era (2003).

[46] Renyi Zhang et al. “Nucleation and growth of nanoparticles in the atmosphere”. In: *Chemical Reviews* (2012).

[47] Renyi Zhang et al. “Formation of urban fine particulate matter”. In: *Chemical Reviews* (2015).

[48] Monica Bucciantini et al. “Inherent toxicity of aggregates implies a common mechanism for protein misfolding diseases”. In: *Nature* (2002).

[49] Dominic M. Walsh et al. “Naturally secreted oligomers of amyloid beta protein potently inhibit hippocampal long-term potentiation in vivo”. In: *Nature* (2002).

[50] Christian Haass and Dennis J. Selkoe. “Soluble protein oligomers in neurodegeneration: lessons from the Alzheimer’s amyloid beta-peptide”. In: *Nature Reviews. Molecular Cell Biology* (2007).

[51] Georg Meisl et al. “Differences in nucleation behavior underlie the contrasting aggregation kinetics of the Aβ40 and Aβ42 peptides”. In: *Proceedings of the National Academy of Sciences* (2014).

[52] Georg Meisl et al. “Quantitative analysis of intrinsic and extrinsic factors in the aggregation mechanism of Alzheimer-associated Aβ-peptide”. In: *Scientific Reports* (2016).

[53] Ricardo Gaspar et al. “Secondary nucleation of monomers on fibril surface dominates α-synuclein aggregation and provides autocatalytic amyloid amplification”. In: *Quarterly Reviews of Biophysics* (2017).

[54] “Fiber-dependent amyloid formation as catalysis of an existing reaction pathway”. In: *Proceedings of the National Academy of Sciences* (2007).

[55] Erik Hermansson et al. “The chaperone domain BRICHOS prevents CNS toxicity of amyloid-β peptide in Drosophila melanogaster”. In: *Disease Models & Mechanisms* (2014).

[56] Thomas C. T. Michaels et al. “Dynamics of oligomer populations formed during the aggregation of Alzheimer’s Aβ42 peptide”. In: *Nature Chemistry* (2020).

[57] Yuan Gao et al. “Out-of-Register Parallel β-Sheets and Antiparallel β-Sheets Coexist in 150-kDa Oligomers Formed by Amyloid-β(1-42)”. In: *Journal of Molecular Biology* (2020).

[58] Vijayaraghavan Rangachari et al. “Amyloid-beta(1-42) rapidly forms protofibrils and oligomers by distinct pathways in low concentrations of sodium dodecylsulfate”. In: *Biochemistry* (2007).

[59] Montserrat Serra-Batiste et al. “Aβ42 assembles into specific β-barrel pore-forming oligomers in membrane-mimicking environments”. In: *Proceedings of the National Academy of Sciences* (2016).

[60] Samuel I. A. Cohen et al. “Nucleated polymerization with secondary pathways. II. Determination of self-consistent solutions to growth processes described by non-linear master equations”. In: *The Journal of Chemical Physics* (2011).

[61] Marielle Aulikki Wälti et al. “Atomic-resolution structure of a disease-relevant Aβ(1-42) amyloid fibril”. In: *Proceedings of the National Academy of Sciences of the United States of America* (2016).

[62] Michael T. Colvin et al. “Atomic Resolution Structure of Monomorphic Aβ42 Amyloid Fibrils”. In: *Journal of the American Chemical Society* (2016).

[63] Veronica Lattanzi et al. “Amyloid β 42 fibril structure based on small-angle scattering”. In: *Proceedings of the National Academy of Sciences* (2021).

[64] Matthias Schmidt et al. “Peptide dimer structure in an Aβ(1-42) fibril visualized with cryo-EM”. In: *Proceedings of the National Academy of Sciences of the United States of America* (2015).

[65] Lothar Gremer et al. “Fibril structure of amyloid-β(1–42) by cryo–electron microscopy”. In: *Science* (2017).

[66] Marius Kollmer et al. “Cryo-EM structure and polymorphism of Aβ amyloid fibrils purified from Alzheimer’s brain tissue”. In: *Nature Communications* (2019).

[67] Rui Zhang et al. “Interprotofilament interactions between Alzheimer’s Abeta1-42 peptides in amyloid fibrils revealed by cryoEM”. In: *Proceedings of the National Academy of Sciences of the United States of America* (2009).

[68] *Support — pymol.org*. URL: `https://pymol.org/2/support.html?`.

[69] Ivan Rayment. “Protein Structure”. In: *Encyclopedia of Physical Science and Technology (Third Edition)*. 2003.

[70] W. Kauzmann. “Some factors in the interpretation of protein denaturation”. In: *Advances in Protein Chemistry* (1959).

[71] K. A. Dill. “Dominant forces in protein folding”. In: *Biochemistry* (1990).

[72] John Schellman and Charlotte Schellman. In: *Comprehensive Biochemistry*. 2000.

[73] Huan-Xiang Zhou and Xiaodong Pang. “Electrostatic Interactions in Protein Structure, Folding, Binding, and Condensation”. In: *Chemical reviews* (2018).

[74] Özlem Bahadir Acikara. *Ion-Exchange Chromatography and Its Applications*. IntechOpen, 2013.

[75] David L. Nelson. *Lehninger Principles of Biochemistry*. 6th edition. 2012.

[76] Alfredo Morales. “Quantitative Chemical Analysis 7E Daniel C. Harris”. In: ().

[77] H. Naiki et al. “Fluorometric determination of amyloid fibrils in vitro using the fluorescent dye, thioflavin T1”. In: *Analytical Biochemistry* (1989).

[78] Rafael Fernandez-Leiro and Sjors H. W. Scheres. “Unravelling biological macromolecules with cryo-electron microscopy”. In: *Nature* (2016).

[79] Dmitry Lyumkis. “Challenges and opportunities in cryo-EM single-particle analysis”. In: *The Journal of Biological Chemistry* (2019).

[80] Christian Colliex. “Seeing and measuring with electrons: Transmission electron microscopy today and tomorrow – An introduction”. In: *Comptes Rendus Physique*. Seeing and measuring with electrons: Transmission Electron Microscopy today and tomorrow (2014).

[81] Jacques Dubochet et al. “Cryo-electron microscopy of vitrified specimens”. In: *Quarterly Reviews of Biophysics* (1988).

[82] Ulrike Endesfelder and Mike Heilemann. “Direct Stochastic Optical Reconstruction Microscopy (dSTORM)”. In: *Advanced Fluorescence Microscopy: Methods and Protocols*. 2015.

[83] Sebastian van de Linde et al. “Direct stochastic optical reconstruction microscopy with standard fluorescent probes”. In: *Nature Protocols* (2011).

[84] Samuel I. A. Cohen et al. “Distinct thermodynamic signature of oligomer generation in the aggregation of the amyloid-β peptide”. In: *Nature chemistry* (2018).

[85] Risto Cukalevski et al. “The Aβ40 and Aβ42 peptides self-assemble into separate homomolecular fibrils in binary mixtures but cross-react during primary nucleation”. In: *Chemical Science* (2015).

[86] F. A. Ferrone, J. Hofrichter and W. A. Eaton. “Kinetics of sickle hemoglobin polymerization. II. A double nucleation mechanism”. In: *Journal of Molecular Biology* (1985).

[87] Vito Foderà et al. “Secondary Nucleation and Accessible Surface in Insulin Amyloid Fibril Formation”. In: *The Journal of Physical Chemistry B* (2008). Publisher: American Chemical Society.

[88] Alexander K. Buell et al. “Solution conditions determine the relative importance of nucleation and growth processes in α-synuclein aggregation”. In: *Proceedings of the National Academy of Sciences* (2014).

[89] Georg Meisl et al. “Modulation of electrostatic interactions to reveal a reaction network unifying the aggregation behaviour of the Aβ42 peptide and its variants”. In: *Chemical Science* (2017).

[90] Erik Portelius et al. “Identification of novel APP/Abeta isoforms in human cerebrospinal fluid”. In: *Neuro-Degenerative Diseases* (2009).

[91] Alfred T. Welzel et al. “Secreted amyloid β-proteins in a cell culture model include N-terminally extended peptides that impair synaptic plasticity”. In: *Biochemistry* (2014).

[92] Naoki KANEKO et al. “Identification and quantification of amyloid beta-related peptides in human plasma using matrix-assisted laser desorption/ionization time-of-flight mass spectrometry”. In: *Proceedings of the Japan Academy. Series B, Physical and Biological Sciences* (2014).

[93] Pauline Bros et al. “Quantitative detection of amyloid-β peptides by mass spectrometry: state of the art and clinical applications”. In: *Clinical Chemistry and Laboratory Medicine (CCLM)* (2015).

[94] Olga Szczepankiewicz et al. “N-Terminal Extensions Retard Aβ42 Fibril Formation but Allow Cross-Seeding and Coaggregation with Aβ42”. In: *Journal of the American Chemical Society* (2015).

[95] Tanja Weiffert et al. “Increased Secondary Nucleation Underlies Accelerated Aggregation of the Four-Residue N-Terminally Truncated Aβ42 Species Aβ5–42”. In: *ACS Chemical Neuroscience* (2019).

[96] C. Dammers et al. “Pyroglutamate-modified Aβ(3-42) affects aggregation kinetics of Aβ(1-42) by accelerating primary and secondary pathways”. In: *Chemical Science* (2017).

[97] Kalyani Sanagavarapu et al. “Specific Sequence of the flexible N-terminal tail plays a key role in secondary nucleation of Ab42. (In preparation)”.

[98] Giuseppe Di Fede et al. “A recessive mutation in the APP gene with dominant-negative effect on amyloidogenesis”. In: *Science (New York, N.Y.)* (2009).

[99] Thorlakur Jonsson et al. “A mutation in APP protects against Alzheimer’s disease and age-related cognitive decline”. In: *Nature* (2012).

[100] Iryna Benilova et al. “The Alzheimer Disease Protective Mutation A2T Modulates Kinetic and Thermodynamic Properties of Amyloid-β (Aβ) Aggregation”. In: *Journal of Biological Chemistry* (2014).

[101] J. C. Janssen et al. “Early onset familial Alzheimer’s disease: Mutation frequency in 31 families”. In: *Neurology* (2003).

[102] Kenjiro Ono, Margaret M. Condron and David B. Teplow. “Effects of the English (H6R) and Tottori (D7N) Familial Alzheimer Disease Mutations on Amyloid β-Protein Assembly and Toxicity”. In: *The Journal of Biological Chemistry* (2010).

[103] Y. Wakutani et al. “Novel amyloid precursor protein gene missense mutation (D678N) in probable familial Alzheimer’s disease”. In: *Journal of Neurology, Neurosurgery, and Psychiatry* (2004).

[104] Wei-Ting Chen et al. “Amyloid-beta (Aβ) D7H mutation increases oligomeric Aβ42 and alters properties of Aβ-zinc/copper assemblies”. In: *PloS One* (2012).

[105] Kalyani Sanagavarapu et al. “N-terminal sequence determinants of secondary nucleation (In preparation)”.

[106] L. Hendriks et al. “Presenile dementia and cerebral haemorrhage linked to a mutation at codon 692 of the beta-amyloid precursor protein gene”. In: *Nature Genetics* (1992).

[107] Vicki Betts et al. “Aggregation and catabolism of disease-associated intra-Aβ mutations: reduced proteolysis of AβA21G by neprilysin”. In: *Neurobiology of disease* (2008).

[108] Kazuma Murakami et al. “Synthesis, aggregation, neurotoxicity, and secondary structure of various A beta 1-42 mutants of familial Alzheimer’s disease at positions 21-23”. In: *Biochemical and Biophysical Research Communications* (2002).

[109] Alexis Huet and Philippe Derreumaux. “Impact of the mutation A21G (Flemish variant) on Alzheimer’s beta-amyloid dimers by molecular dynamics simulations”. In: *Biophysical Journal* (2006).

[110] Xiaoting Yang et al. “On the role of sidechain size and charge in the aggregation of Aβ42 with familial mutations”. In: *Proceedings of the National Academy of Sciences of the United States of America* (2018).

[111] E. Levy et al. “Mutation of the Alzheimer’s disease amyloid gene in hereditary cerebral hemorrhage, Dutch type”. In: *Science (New York, N.Y.)* (1990).

[112] K. Kamino et al. “Linkage and mutational analysis of familial Alzheimer disease kindreds for the APP gene region”. In: *American Journal of Human Genetics* (1992).

[113] C. Nilsberth et al. “The ’Arctic’ APP mutation (E693G) causes Alzheimer’s disease by enhanced Abeta protofibril formation”. In: *Nature Neuroscience* (2001).

[114] Orso Bugiani et al. “Hereditary cerebral hemorrhage with amyloidosis associated with the E693K mutation of APP”. In: *Archives of Neurology* (2010).

[115] T. J. Grabowski et al. “Novel amyloid precursor protein mutation in an Iowa family with dementia and severe cerebral amyloid angiopathy”. In: *Annals of Neurology* (2001).

[116] María Pagnon de la Vega et al. “The Uppsala APP deletion causes early onset autosomal dominant Alzheimer’s disease by altering APP processing and increasing amyloid β fibril formation”. In: *Science Translational Medicine* (Aug. 2021).

[117] Gabriel A. Braun et al. *The Amyloid β peptide 37, 38 and 40 individually and cooperatively inhibit amyloid-β 42 aggregation (In preparation).*

[118] Samuel J. Bunce et al. “Molecular insights into the surface-catalyzed secondary nucleation of amyloid-β40 (Aβ40) by the peptide fragment Aβ16–22”. In: *Science Advances* (2019).

[119] Kalyani Sanagavarapu et al. “On the role of phosphorylation of serine residues in aggregation mechanism of amyloid beta-peptide. (In preparation)”.

[120] Manuela R. Zimmermann et al. “Mechanism of Secondary Nucleation at the Single Fibril Level from Direct Observations of Aβ42 Aggregation”. In: *Journal of the American Chemical Society* (2021).

[121] Mattias Törnquist and Sara Linse. “Chiral Selectivity of Secondary Nucleation in Amyloid Fibril Propagation”. In: *Angewandte Chemie* (2021).